Journal of Building Engineering 85 (2024) 108674

Contents lists available at ScienceDirect

Journal of Building Engineering

journal homepage: www.elsevier.com/locate/jobe

Optimum tuned mass damper inerter under near-fault pulse-like ground motions of buildings including soil-structure interaction

Said Elias [b,*], Salah Djerouni [a]

[a] Laboratoire de Génie Energétique et Matériaux, LGEM, Université de Biskra, B.P. 145, R.P. 07000, Biskra, Algeria
[b] Marie Skłodowska-Curie Actions (MSCA), Institute for Risk and Reliability, Leibniz University Hannover (LUH), Hannover, Germany

ARTICLE INFO

Keywords:
Building
Earthquake
Tuned mass damper inerter (TMDI)
Soil structure interaction (SSI)
Seismic resilience
Multi-degree of freedom (MDOF)
Optimization methods

ABSTRACT

This study investigates the effectiveness of the tuned mass damper inerter (TMDI) in mitigating building response, considering the soil structure interaction (SSI). Three types of models are examined: single degree of freedom (SDOF), low-rise multi-degree of freedom (MDOF), and high-rise MDOF. Additionally, the natural period of the SDOF model is varied to explore the TMDI's efficacy across different ranges. Frequency and time domain analysis are conducted under pulse-like ground motions. The H_2 and genetic algorithm (GA) are used to optimize the parameters of the TMDI. In this optimization method the transfer function for displacement response is minimized. In time domain analysis we used Newmark's integration method to solve the equation of motion for all the cases considered. It is found that the optimized TMDI proves highly effective in mitigating the displacement response of the buildings, accounting for SSI. Notably, its efficiency is more pronounced when pulse period aligns closely with the buildings' natural period. In addition, a notable pattern emerges, wherein the TMDI excels in mitigating response for buildings experiencing large motion, thereby enhancing safety under severe conditions. These findings offer valuable insights into the application and optimization of the TMDI to enhance seismic performance in various buildings, while considering complex interaction with the soil.

1. Introduction

Natural hazards such as earthquakes and wind cause undesirable vibrations in different civil structures. Hence, researchers and practice engineers proposed and implemented different vibration absorbers such as active, passive, semi-active, and hybrid for dynamical response mitigation of civil structures. Passive vibration absorbers are more ideal than others as they are affordable and reliable. Tuned mass dampers (TMDs) are well-known among passive vibration absorbers, and are used in many real-life structures, especially wind response mitigation of high-rise buildings [1]; seismic response mitigation [2–5], seismic response mitigation by consideration of soil structure interaction (SSI) [6], pedestrian bridges [7,8], and railway bridges [9,10].

It is a common understanding that the TMDs are quite sensitive to frequency detuning, therefore that requires considering the robustness in the design of such devices. Hence, noticeably the research in the recent decades has been focused on the optimization of TMDs [11–14]. For example, in their study, Cao and Li [12] introduced the tuned tandem mass dampers-inerters (TTMDI) as a groundbreaking control device, amalgamating tuned tandem mass dampers with two inerters. The TTMDI showcases outstanding performance, marked by high effectiveness and wide frequency spacing, while prioritizing simplicity and ease of implementation. The

* Corresponding author. Marie Skłodowska-Curie Actions (MSCA), Institute for Risk and Reliability, Leibniz University Hannover (LUH), Hannover, Germany.
E-mail address: elias.rahimi@irz.uni-hannover.de (S. Elias).

https://doi.org/10.1016/j.jobe.2024.108674
Received 29 July 2023; Received in revised form 9 January 2024; Accepted 28 January 2024
Available online 6 February 2024

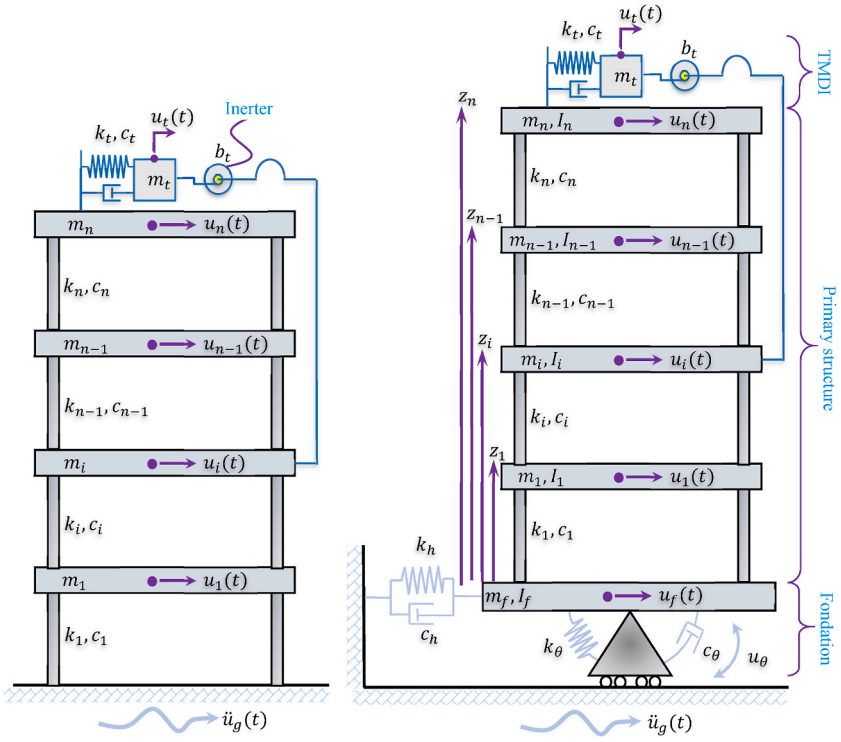

Fig. 1. Schematic of controlled MDOF structure equipped with TMDI on top (right) including SSI effect and (left) with ignoring SSI effect (fixed base) subjected to ground motion.

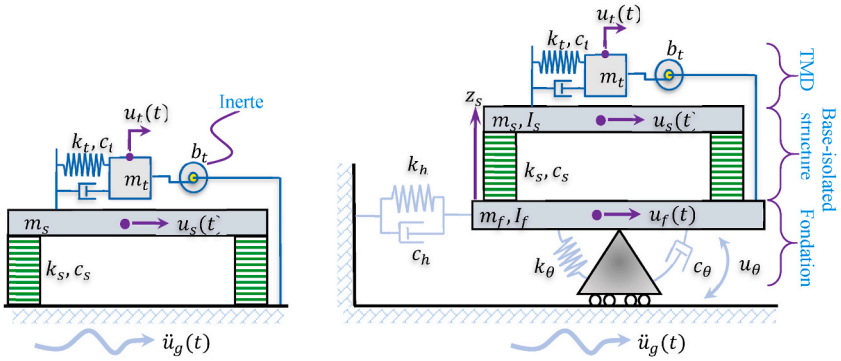

Fig. 2. Schematic of controlled SDOF structure equipped with grounded TMDI (right) including SSI effect and (left) with ignoring SSI effect (fixed base) subjected to ground motion.

authors conducted thorough evaluations, examining the TTMDI's effectiveness, strokes, stiffness, damping coefficient, inertance coefficient distributions, frequency spacing, and frequency response. The collective findings assert the TTMDI's superiority over traditional control devices. In addition, scientists typically focused on the effects of external forces [15–17], the mass ratio of TMD [18–20], uncertainty of the damped main system [21–23], and optimization techniques [24–26] on the optimum parameters of TMDs. Mainly the parent structures have been assumed to be single degree of freedom (SDOF) system.

Joshi and Jangid [27] compared the efficiency of the single TMD with MTMDs in dynamic response mitigation of a building structure subjected to white noise excitations. Sadek et al. [28] recommended a procedure of approximating the optimal design parameters of TMDs for the decrease of vibrations in multi-floor buildings under earthquakes. The method was successful and adopted by many researchers for vibration control of damped structures. Hadi and Arfadi [29] studied the impact of TMDs in decreasing the peak top floor displacement of a ten-floor building subjected to earthquakes. Genetic algorithm (GA) was used to get the optimal parameters of the TMD. A detailed literature survey was presented by Elias and Matsagar [30]. Bekdaş et al. [31] evaluated the optimal parameters of TMD by employing the bat optimization algorithm. They used the harmony search algorithm to obtain the optimum parameters. The method was effective in decreasing vibrations in multi-floor buildings under earthquakes. Yucel et al. [32] studied the effect of using

Table 1
Dynamic parameters of 5-story building examined in this study [75,68].

No. of stories (n)	5
Story height (z_i)	4 m
Story mass (m_i)	300 t
Story moment of inertia (I_i)	7.5×10^6 kg m^2
Story stiffness (k_i)	$k_i = 7k, 5k, 3k, 2k$ and k ; $k = 50$ $(MN\ /m)$
Foundation radius (R_f)	10 m
Foundation mass (m_f)	500 t
Foundation moment of inertia (I_f)	2.083×10^6 kg m^2

Table 2
Dynamic parameters of 40-story building examined in this study [52–57].

No. of stories (n)	40
Story height (z_i)	4 m
Story mass (m_i)	9.81×10^2 t
Story moment of inertia (I_i)	1.31×10^8 kg m^2
Story stiffness (k_i)	$k_1 = 2130$ $(MN\ /m)$ $k_{40} = 998$ $(MN\ /m)$ $k_{40} \leq k_i \leq k_1$
Story stiffness (c_i)	$c_1 = 19.96$ $(MN\,s\,/m)$ $c_{40} = 42.6$ $(MN\,s\,/m)$ $c_{40} \leq c_i \leq c_1$
Foundation radius (R_f)	20 m
Foundation mass (m_f)	1.96×10^3 t
Foundation moment of inertia (I_f)	1.96×10^6 kg m^2

Table 3
Parameters of the considered soil types [75,68].

Soil type	$V_s[m/s]$	$\rho[kg/m^3]$	$G[MN/m^2]$	ν
Soft soil	100	1800	18	0.49
Medium soil	300	1900	171	0.48
Dense soil	500	2400	600	0.33

optimal TMD in reducing the peak displacements of the buildings under various earthquakes. Araz and Kahya [33] evaluated the control performances of a single optimal TMD and series tuned mass dampers (STMD) to reduce the vibrations of buildings under earthquakes. It is commonly noted that efficiency of TMDs improves with the TMD mass. Nonetheless, it is practically not convenient to attach and support a heavy TMD mass in building structures. This practical constraint of TMDs can be improved to some magnitude by utilizing unique devices named inerters. Inerters are the devices that can generate inertia forces relative to the ground acceleration they are subjected to Ref. [34]. The TMD with an inerter can produce great inertia forces with significantly little physical mass. A TMD attached with an inerters are known as Tuned Mass Damper Inerters (TMDI). Marian and Giaralis [35] showed one of the first solutions for optimal TMDIs to control the vibrations of SDOF systems under harmonic base excitation. Marian and Giaralis [36] assessed the optimum design of TMDIs under white noise excitations. Taflanidis et al. [37] assessed three different kinds of inerter dampers (ID), such as tuned viscous mass damper (TVMD), tuned mass damper inerter (TMDI), and tuned inerter damper (TID). The IDs were discovered to be efficient in earthquake response mitigation of structures. Petrini et al. [38] investigated the efficiency of the TMDI in response mitigation of a benchmark structure. They performed an innovative technique to optimize the parameters of the TMDI by minimizing the floor response (accelerations) produced by the wind. Lately, multiple TMDI have been investigated for response

Table 4
Damping coefficient and stiffness for soil types considered in this study [52,57,75].

Building	Soil type	$c_h[MN\,s\,/m]$	$c_\theta[MN\,s\,/m]$	$k_h[MN\ /m]$	$k_\theta[MN\ /m]$
five-story	Soft soil	5.48×10^1	1.41×10^7	9.54×10^6	9.41×10^8
	Medium soil	1.73×10^2	4.39×10^7	9.00×10^7	8.77×10^9
	Dense soil	3.31×10^2	7.16×10^7	2.87×10^8	2.39×10^{10}
forty-story	Soft soil	2.19×10^2	2.26×10^8	1.91×10^7	7.53×10^9
	Medium soil	6.90×10^2	7.02×10^8	1.80×10^8	7.02×10^{10}
	Dense soil	1.32×10^7	1.15×10^9	5.75×10^8	1.91×10^{11}

Table 5
TMDI ranges of optimization.

Frequency ratio	Min	Max	Damping ratio	Min	Max
υ_t	0.5	1.2	ξ_t	0.1	0.8

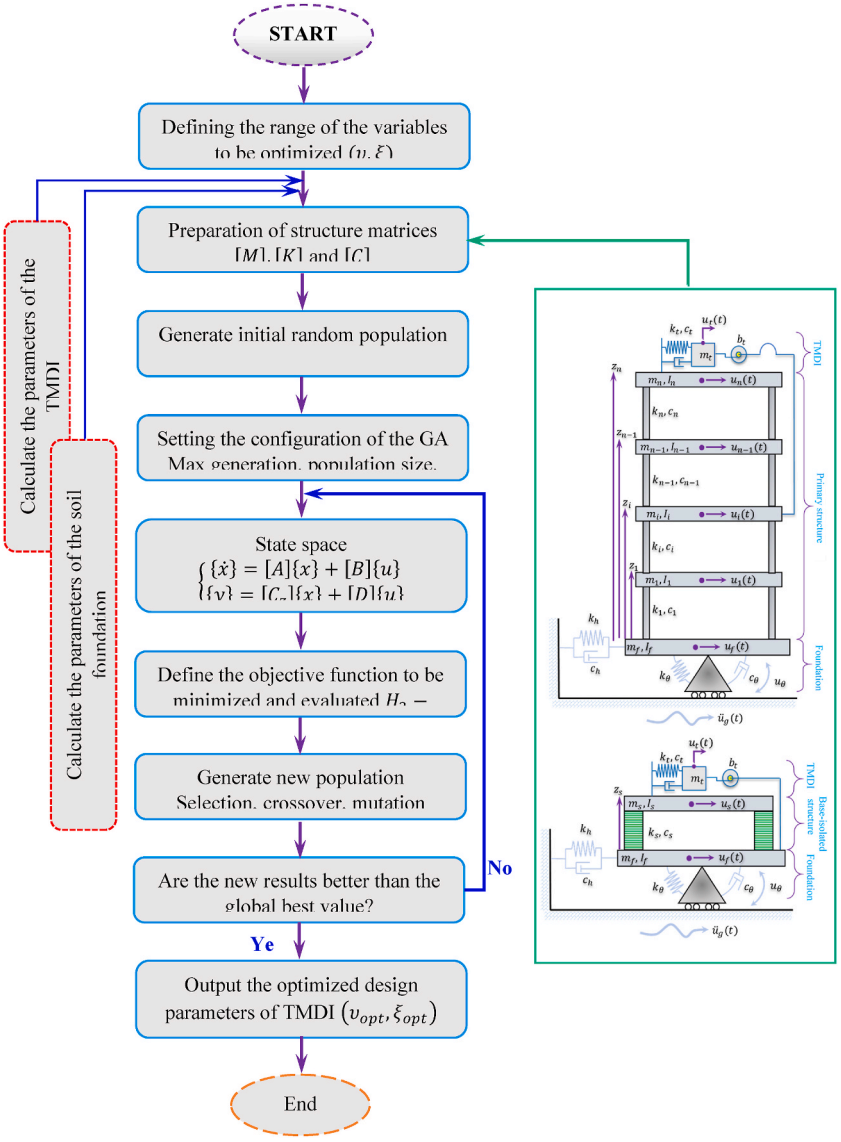

Fig. 3. Optimization Process Flowchart: Enhancing Tuned Mass Damper Inerter (TMDI) with Soil-Structure Interaction using H2 and Genetic Algorithm (GA).

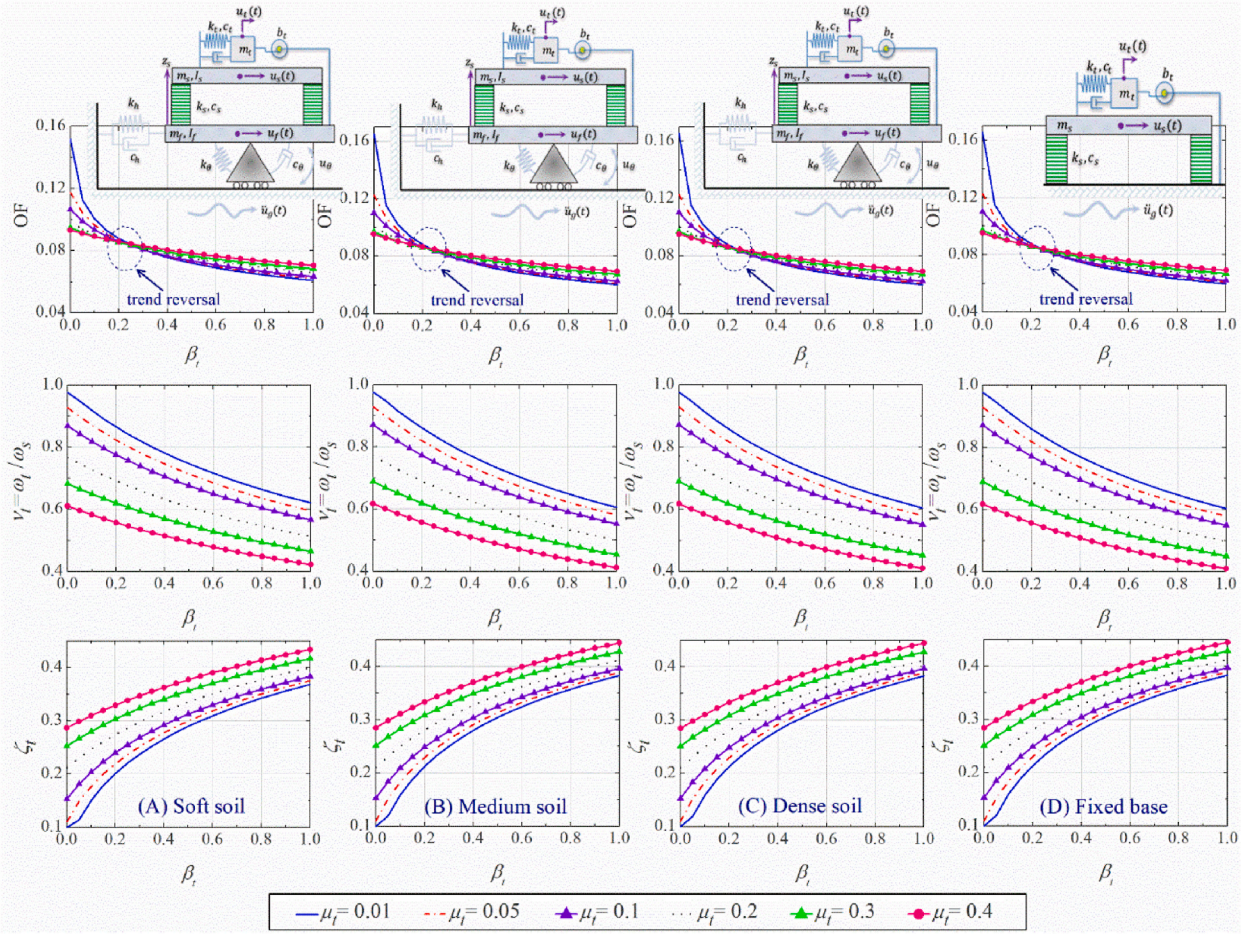

Fig. 4. Minimizing the objective function (OF), variation frequency ratio and variation damping ratio, with respect to the variation of inertance ratio.

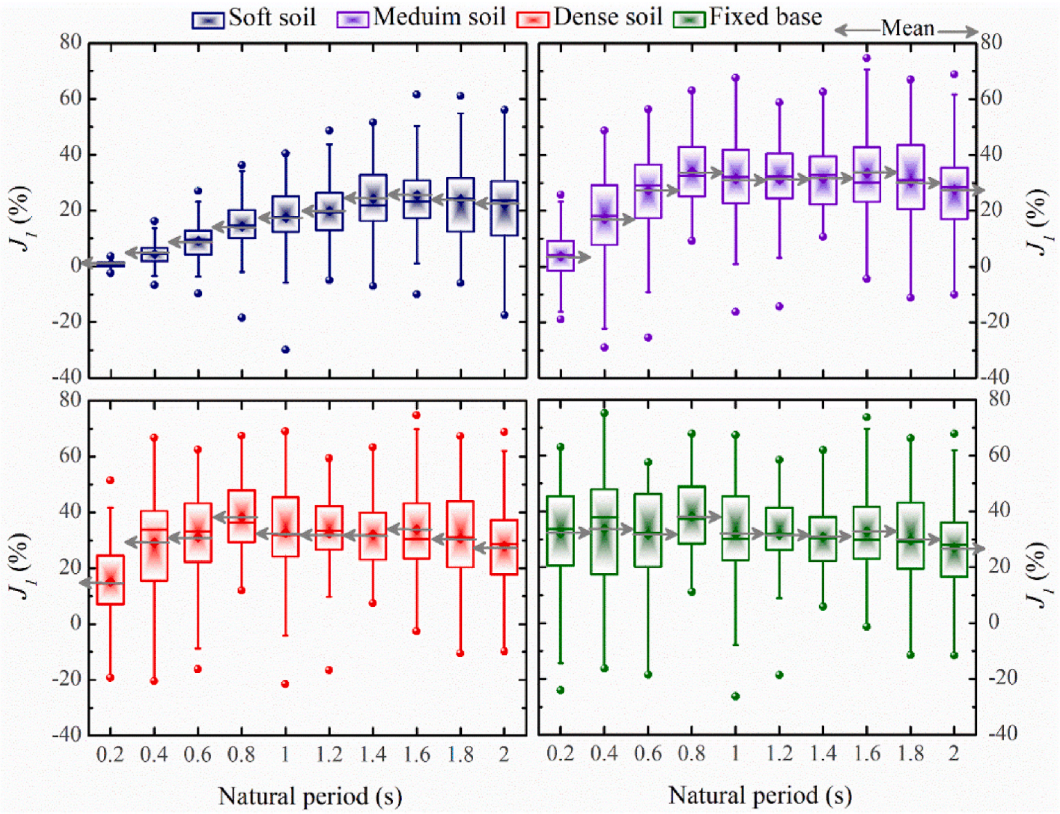

Fig. 5. Variation of J_1 of SDOF with different soil properties under pulse-like ground motions records. The results correspond for a periods from 0.2 to 2s.

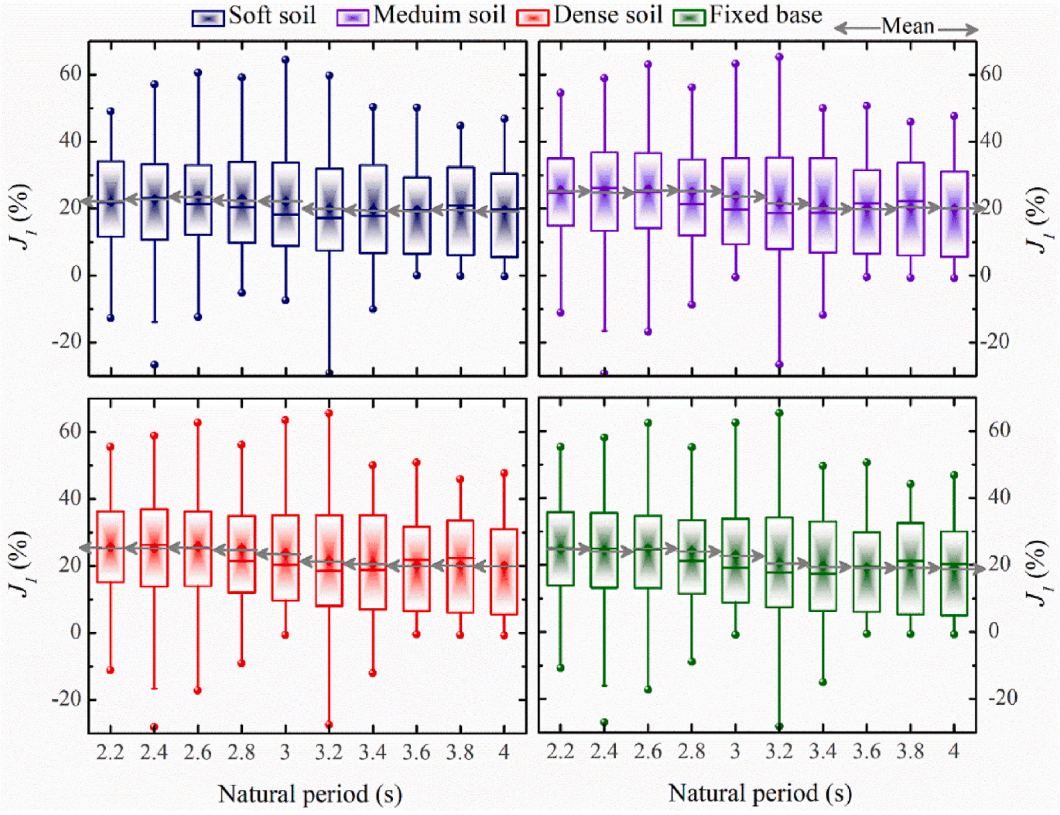

Fig. 6. Variation of J_1 of SDOF with different soil properties and under pulse-like ground motions records. The results correspond to a range of periods from 2.2 to 4s.

mitigation of structures [39,40]. Double-mass TMDI for mitigation of seismic response of buildings has recently been reported in the literature [41].

In the literature, negative stiffness and inerter dampers were compared for their vibration isolation performance [42]. The fixed-point theory was utilized to derive optimal parameters for the SDOF system equipped with the combination of inerter and NSD for seismic protection [43–46]. A unified study of multimode damping effects of negative stiffness and inerter mechanisms was performed when paired with a viscous damper for cable vibration control [47]. In their work, Islam and Jangid [48–50] demonstrated the efficacy of negative stiffness and inerter dampers in enhancing the vibration response of various structures under earthquake excitations. The study [50] specifically delved into optimizing parameters and assessing the performance of dampers based on negative stiffness and inerter mechanisms for structures employing base isolation techniques.

Generally, the earlier investigations (discussed above) ignored the SSI effect as the researchers believed that the foundation for civil structure was built strong. However, Elias [51] concluded that the soil type significantly influenced the design parameters of the vibration absorber schemes and seismic response of the structure. Because the SSI substantially shifts the frequencies of the structure, it is critical to consider the SSI effect in the optimum design of the TMD. It is reported that the previous investigations typically vary based on the optimization techniques [52–54], the earthquake fault type [55–57] and the objective functions [58,59]. Zhang et al. [60] studied the nonlinear fragility estimation of a 20-floor steel building equipped with TMD and considering SSI under earthquakes. They noted that the single TMD can remarkably reduce the structural demands, while the SSI impacts can increase the fragility of the building structures, particularly if subjected to strong earthquakes. Other investigators also have explored the efficiency of multiple TMDs (MTMDs) [61–63], inerter TMD (TMDI) [64], and particle TMDs [65] in decreasing earthquake vibrations of tall buildings counting the SSI effects. Wang and Lin [61] concluded that by suitably increasing the frequency spacing of the optimal MTMDs, the detuning effect were reduced. Li and Han [62] reported that the dominant ground frequency and SSI have substantial effect on the optimum parameters, stroke, and efficiency of the MTMDs. Non-optimal positioning of MTMDS on a floor was found to have the potential of reducing damping efficiency and amplifying peak response while SSI effect is considered [63]. Generally, it is noted that mostly a single TMD is used to reduce the seismic response of buildings with SSI effect included. The research on multiple TMDs in response mitigation of such buildings is very limited [66]. Although, for other recently identified structures, the study [67] has revealed noteworthy outcomes concerning the implementation of multiple Tuned Mass Dampers (TMDs), particularly in distributed configurations. The findings suggest that this strategic use of TMDs has led to substantial decreases in structural response under the combined influence of various dynamic loads. Notably, in fixed base systems (without Soil-Structure Interaction, or SSI), and even more significantly in flexible base systems (with SSI), the study underscores the potential effectiveness of employing multiple TMDs,

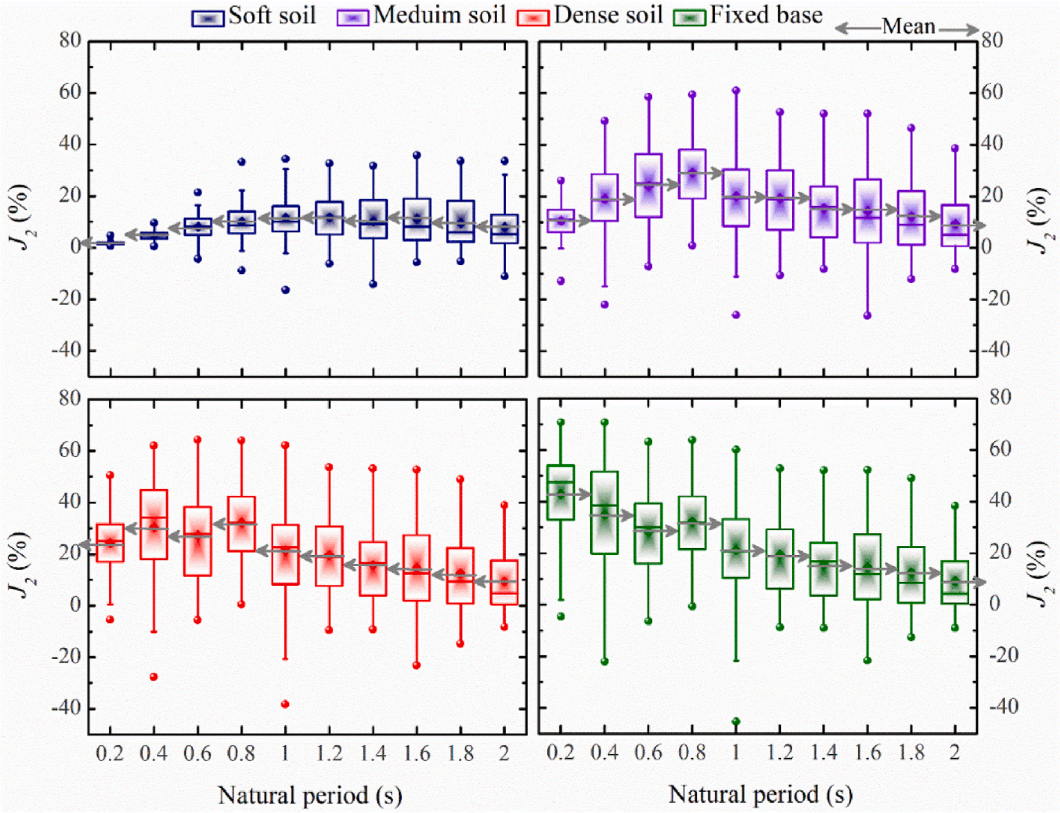

Fig. 7. Variation of J_2 of SDOF with different soil properties and under pulse-like ground motions records. The results correspond for a range of periods from 0.2 to 2s.

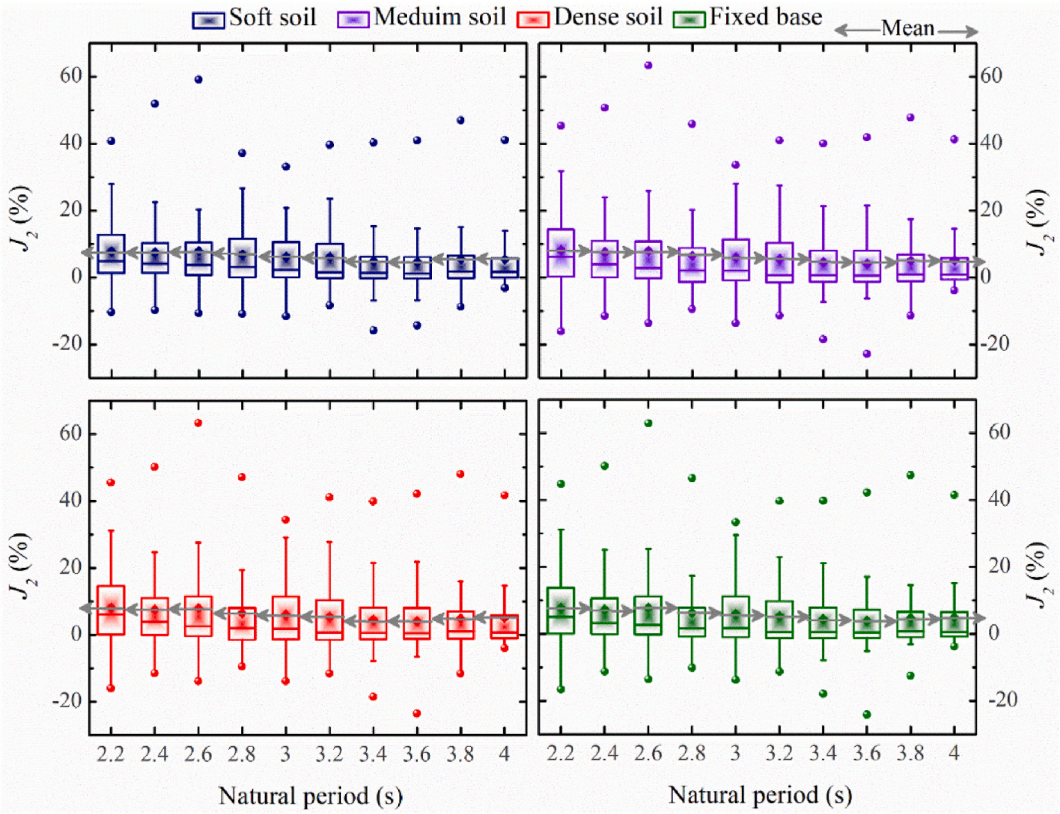

Fig. 8. Variation of J_2 of SDOF with different soil properties and under pulse-like ground motions records. The results correspond to a range of periods from 2.2 to 4s.

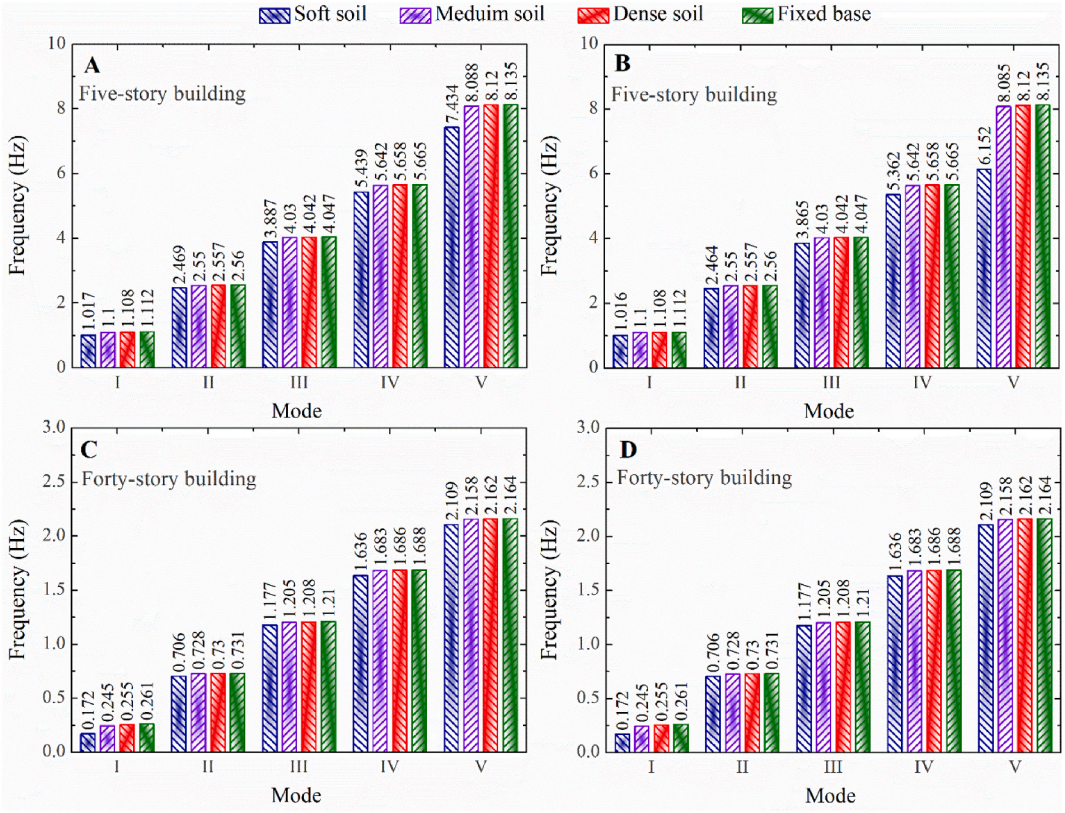

Fig. 9. Main natural frequencies of the low-rise-five story building foundation system and high-rise-forty story building foundation system at different soil type; (A,C) previous study [75], (B,D) present study.

Table 6
Optimum TMDI parameters for low-rise five-story building.

Variables	Soft soil	Medium soil	Dense soil	Fixed base
υ_t	0.980	0.969	0.966	0.965
ξ_t	0.223	0.292	0.298	0.301
μ_t	0.005	0.005	0.005	0.005
β_t	0.2	0.2	0.2	0.2
m_t (t)	7.5	7.5	7.5	7.5
b_t (t)	300	300	300	300
k_t (MN/m)	12.029	13.806	13.904	13.955
c_t (MN s/m)	0.858	1.204	1.233	1.247

especially when distributed, as a promising strategy for minimizing dynamic responses in structures facing combined wind and wave forces.

The existing literature on MTMDs mainly focused on the SSI effect on the effectiveness of the MTMDs or placement effects on the efficiency of MTMDs. However, the effect of the optimum inerter TMDs on the vibration mitigation of SDOF and MDOF by including the SSI effect has not yet been investigated. Moreover, the earthquakes considered in the previous studies (with SSI) were chosen either among the earthquakes with historical importance or among the near-fault and far-fault earthquakes. However, the effect of pulse type earthquake ground motion on the effectiveness of TMDI considering SSI effect has not been earlier assessed. Accordingly, this study intends to fill these gaps in the literature. Therefore, a numerical solution is first developed for achieving earthquake responses of buildings equipped with TMDI including SSI. The H_2 is recommended for the optimization of TMDs by reducing the largest amplitude of the building displacement.

2. Governing equations of motions of structure with SSI

The equation of motion that represent the motion of *n*-DOF structure equipped with TMDI and subject to earthquake excitation can be expressed as:

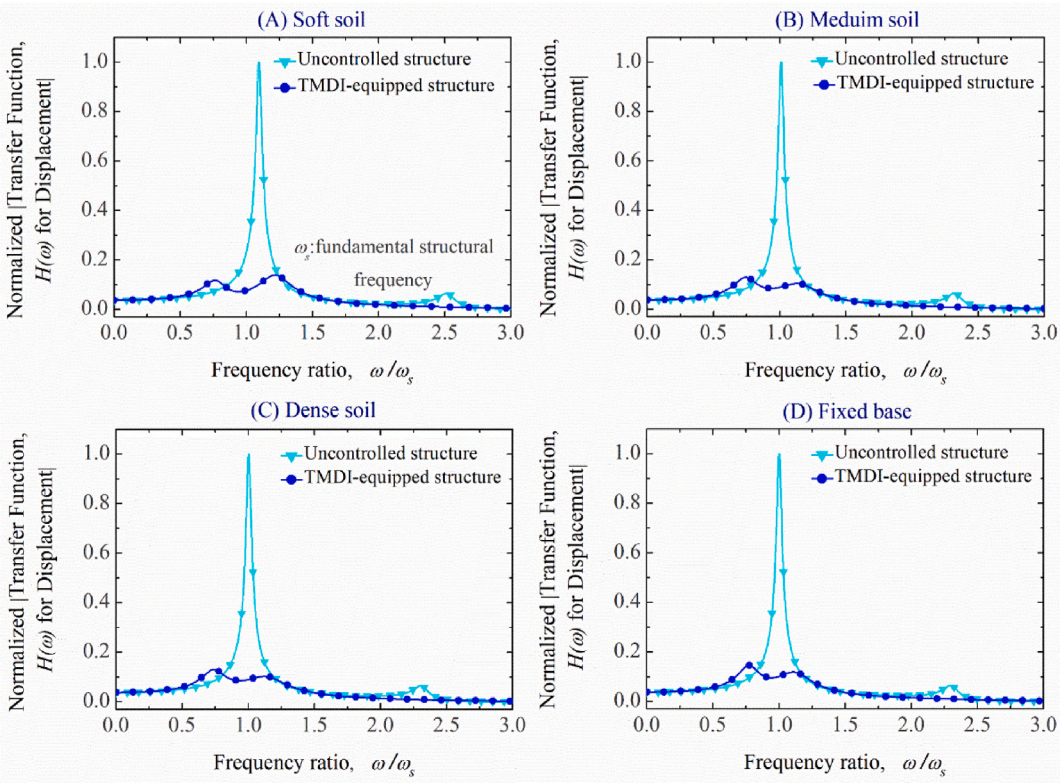

Fig. 10. Transfer function curves $[H(\omega)]$ of the displacement for five-story uncontrolled building and controlled with TMDI, considering different variable soil conditions.

$$[M_t]\ddot{u}_t(t) + [C_t]\dot{u}_t(t) + [K_t]u_t(t) = -F(t) \tag{1}$$

where $M_t, C_t,$ and K_t respectively represent the structural mass, damping, and stiffness matrices of the oscillating system. $\ddot{u}_t, \dot{u}_t$ and u_t respectively denote the relative acceleration, velocity, and displacement vectors. $F(t)$ denotes the force directly applied to the structure which is produced by the earthquake ground motion. The dimension of the matrices and vectors in Eq. (1) change based on considering or not considering of the SSI effect as well as controlled or no control device.

The mass, damping and stiffness matrices of the structure is presented without control. To represent the soil properties in mass, damping and stiffness matrices, the corresponding values must be embedded into the matrices. An n -story fixed base shear building is shown in Fig. 1 (right). Assuming the parameters of the device on top floor is equal to zero. Idealized mass M_t, damping C_t and stiffness K_t matrices for uncontrolled fixed-based shear building, are given by

$$M_t = \begin{bmatrix} M_{n\times n} & Mr_{n\times 1} & Mz_{n\times 1} \\ r^T M_{1\times n} & r^T Mr + m_f & \sum_{i=1}^{n} m_i z_i \\ z^T M_{1\times n} & \sum_{i=1}^{n} m_i z_i & I_f + \sum_{i=1}^{n} (m_i z_i^2 + I_i) \end{bmatrix}_{(n+2)\times(n+2)} \tag{2}$$

$$C_t = \begin{bmatrix} C_{n\times n} & 0_{n\times 1} & 0_{n\times 1} \\ 0_{1\times n} & c_r & 0 \\ 0_{1\times n} & 0 & c_\theta \end{bmatrix}_{(n+2)\times(n+2)}, K_t = \begin{bmatrix} K_{n\times n} & 0_{n\times 1} & 0_{n\times 1} \\ 0_{1\times n} & k_h & 0 \\ 0_{1\times n} & 0 & k_\theta \end{bmatrix}_{(n+2)\times(n+2)} \tag{3}$$

$$F = \begin{Bmatrix} Mr_{n\times 1} \\ r^T Mr + m_f \\ z^T Mr \end{Bmatrix}_{(n+2)\times 1}, \ddot{u}_t = \begin{Bmatrix} \ddot{u}_{n\times 1} \\ \ddot{u}_f \\ \ddot{\theta} \end{Bmatrix}_{(n+2)\times 1}, \dot{u}_t = \begin{Bmatrix} \dot{u}_{n\times 1} \\ \dot{u}_f \\ \dot{\theta} \end{Bmatrix}_{(n+2)\times 1}, u_t = \begin{Bmatrix} u_{n\times 1} \\ u_f \\ \theta \end{Bmatrix}_{(n+2)\times 1} \tag{4}$$

$$u_i^{tot} = u_i + u_f + u_g + u_{r,i} \tag{5}$$

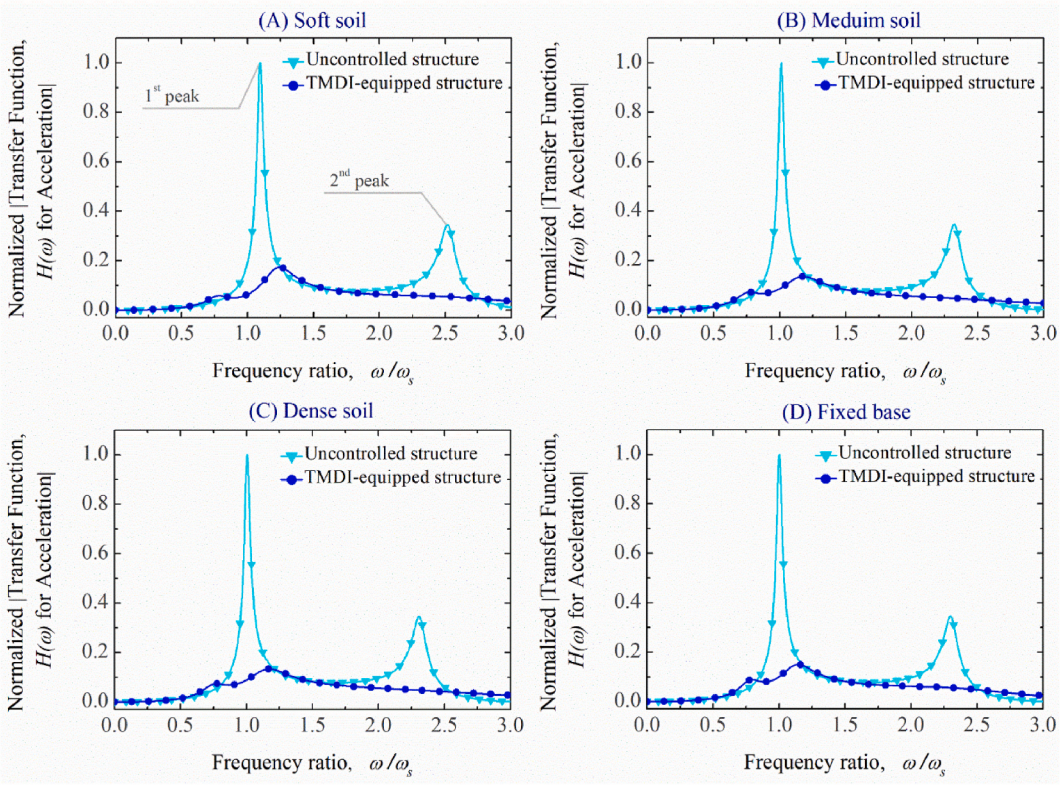

Fig. 11. Transfer function curves $[H(\omega)]$ of the acceleration for five-story uncontrolled building and controlled with TMDI, considering different variable soil conditions.

where M, C, and K are the $((n+2)\times(n+2))$ mass, damping and stiffness matrices of the structural system (host structure), respectively; r is a unit vector with dimension $(n\times 1)$;the absolute height of stories with respect to foundation (ground) is defined with z_i for i^{th} story; m_i, c_i, k_i and I_i are the mass, damping, stiffness and the moment of inertia of each story, respectively. u_i, u_f and θ are displacement of the i^{th} floor of the building, the displacement and the rotation of the foundation, respectively. m_f and I_f are the mass and the moment of the foundation, respectively. The swaying damping, the rocking damping, the swaying stiffness, and the rocking stiffness of soil are represented with c_r, c_θ, k_h and k_θ, respectively. The soil foundation system was modeled by considering it as a viscous dashpot and linear spring system. A node it added to the system and given rotational and translation degrees of freedom corresponding to the soil foundation system. The frequency independent factors give the translation and rocking stiffnesses, and the damping at the node. These factors in turn depend on foundation properties and the soil. The damping and stiffness factors of the soil foundation system considering the soil with shear wave velocity (V_s), shear modulus of elasticity (G), radius of foundation (R), and Poisson's ratio (ν) are [68,69]:

$$c_h=\frac{4.6GR^2}{(2-\nu)V_s}, c_\theta=\frac{0.4GR^4}{(1-\nu)V_s}, k_h=\frac{8GR}{2-\nu}, k_\theta=\frac{8GR^3}{3(1-\nu)} \tag{6}$$

In which c_h and c_θ respectively, refer the horizontal and rocking damping coefficient for the radiation soil damping of the soil-foundation system, k_h and k_θ respectively represent the horizontal and rocking stiffness coefficients of the soil. Theses depend on the geometry of the foundation and the soil properties. The shear wave velocity of the soil can be given by $V_s=\sqrt{G/\rho}$ where ρ is the density of soil. These factors consider the soil-foundation system properties. In case the structure is installed with the TMDI the mass (M_t), damping (C_t) and stiffness (K_t) matrices are:

$$M_t=\begin{bmatrix} M_{(n+1)\times(n+1)} & Mr_{(n+1)\times 1} & Mz_{(n+1)\times 1} \\ r^T M_{1\times(n+1)} & r^T Mr+m_f+m_t & \sum_{i=1}^{n} m_i z_i + m_t z_n \\ z^T M_{1\times(n+1)} & \sum_{i=1}^{n} m_i z_i & I_f+\sum_{i=1}^{n}\left(m_i {z_i}^2+I_i\right)+m_t {z_n}^2 \end{bmatrix}_{(n+3)\times(n+3)} \tag{7}$$

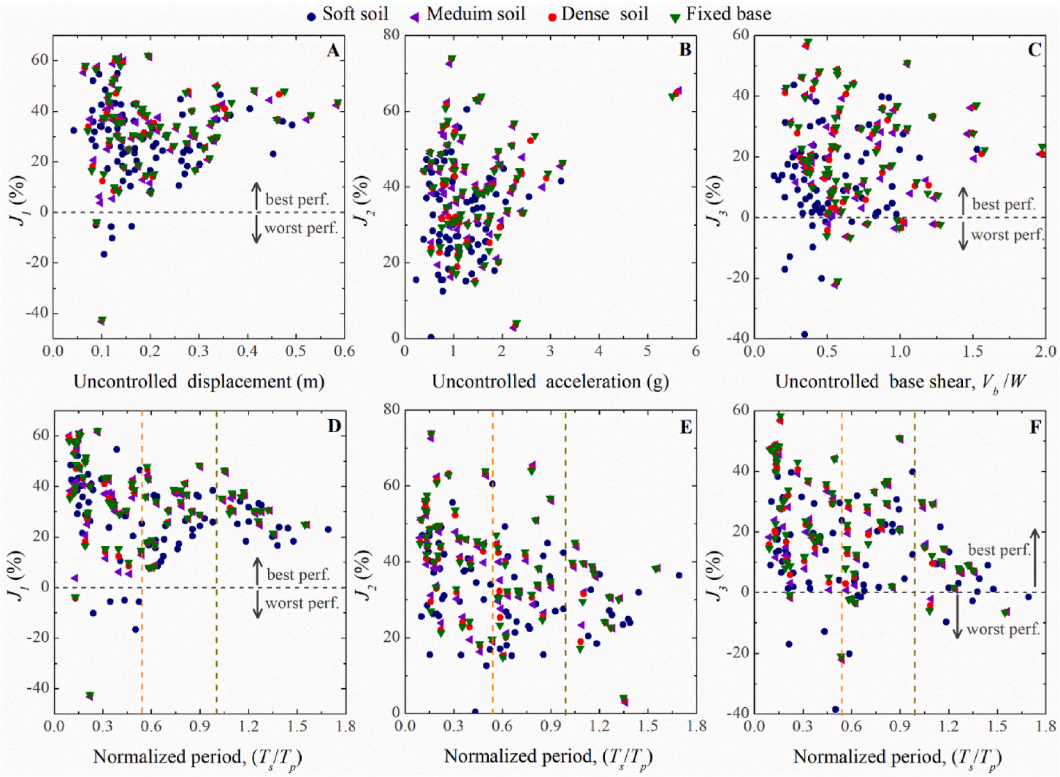

Fig. 12. Variation of J_i with respect to the variation of (A) uncontrolled peak displacement, (B) uncontrolled peak acceleration, (C) uncontrolled normalized base shear, (D, E and F) normalized period (T_s/T_p).The results correspond to low-rise-five-story building.

$$C_t = \begin{bmatrix} C_{(n+1)\times(n+1)} & 0_{(n+1)\times 1} & 0_{(n+1)\times 1} \\ 0_{1\times(n+1)} & c_r & 0 \\ 0_{1\times(n+1)} & 0 & c_\theta \end{bmatrix}_{(n+3)\times(n+3)} \tag{8}$$

$$K_t = \begin{bmatrix} K_{(n+1)\times(n+1)} & 0_{(n+1)\times 1} & 0_{(n+1)\times 1} \\ 0_{1\times(n+1)} & k_h & 0 \\ 0_{1\times(n+1)} & 0 & k_\theta \end{bmatrix}_{(n+3)\times(n+3)} \tag{9}$$

$$F = \begin{Bmatrix} Mr_{n\times 1} \\ r^T Mr + m_f + m_t \\ z^T Mr \end{Bmatrix}_{(n+3)\times 1}, \ddot{u}_t = \begin{Bmatrix} \ddot{u}_{n\times 1} \\ \ddot{u}_f \\ \ddot{\theta} \end{Bmatrix}_{(n+3)\times 1}, \dot{u}_t = \begin{Bmatrix} \dot{u}_{n\times 1} \\ \dot{u}_f \\ \dot{\theta} \end{Bmatrix}_{(n+3)\times 1}$$
$$u_t = \begin{Bmatrix} u_{n\times 1} \\ u_f \\ \theta \end{Bmatrix}_{(n+3)\times 1} \tag{10}$$

where m_t, c_t and k_t are the mass, damping and stiffness of the TMDI passive control device.

3. Numerical examples

In this section first a single degree freedom (SDOF) model is used to numerically test the proposed idea (see Fig. 2). Later, two numerical examples are presented to show the effectiveness of TMDI (see Fig. 1) for vibration mitigation of buildings including the soil structure interaction (SSI). A five-story building is selected to represent the low-rise buildings (see Table 1), and a forty-story building to represent the high-rise buildings (see Table 2). Soil properties for different types of soils are given in Table 3, and the corresponding dynamic properties of the soils are given in Table 4. The near-field pulse-like ground motions chosen for this study are documented in Table A1, with the majority of the records available for download from the source specified in Ref. [70]. These records have been utilized by other researchers to investigate the impact of pulse-like near-field ground motions on various structures [71,72–74]. In order to compare the performance of TMDI in response mitigation of the considered buildings, set of performances criteria such as

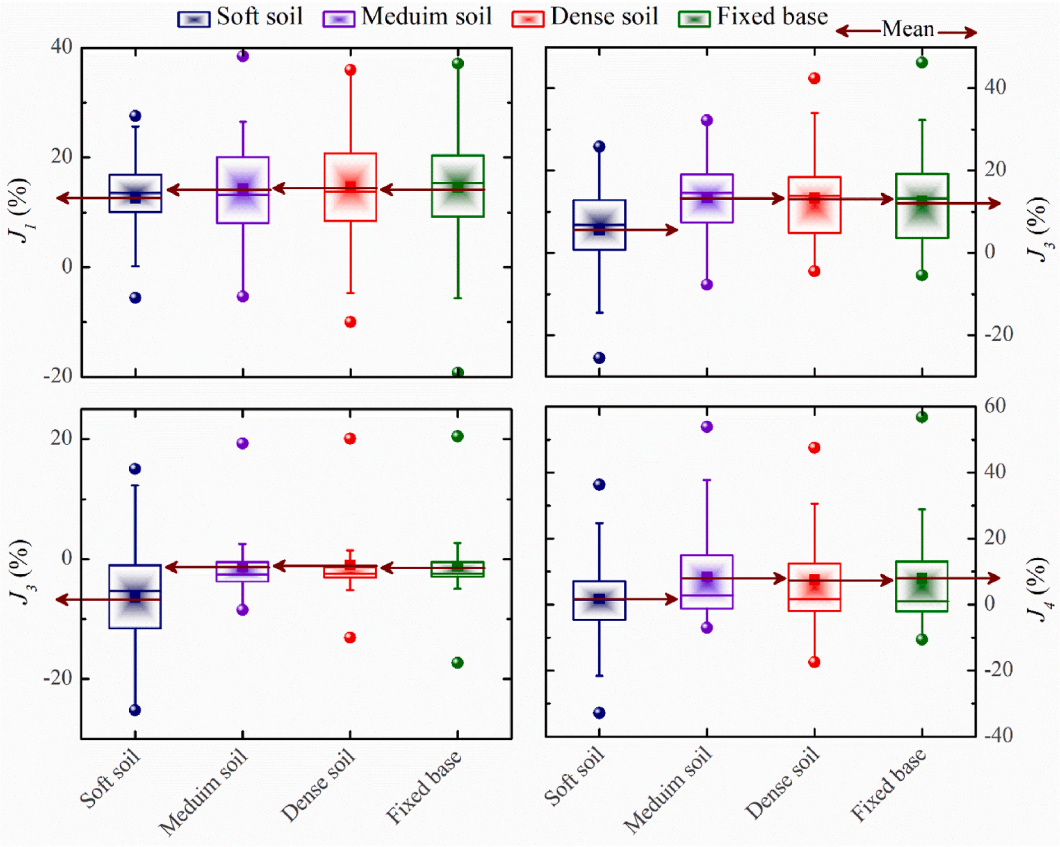

Fig. 13. Box plots representing the distribution of the percentage response reduction data J_1, J_2, J_3 and J_4 for low-rise-five-story building at different variable soil properties and under pulse-like ground motions records.

relative displacement reduction (J_1); absolute acceleration reduction (J_2); base shear reduction (J_3); and reduction of kinetic energy (J_4).

$$J_1 = \frac{u_{nc} - u_c}{u_{nc}} \times 100\% \tag{11}$$

$$J_2 = \frac{\ddot{u}_{nc} - \ddot{u}_c}{\ddot{u}_{nc}} \times 100\% \tag{12}$$

$$J_3 = \frac{V_{b,nc} - V_{b,c}}{V_{b,nc}} \times 100\% \tag{13}$$

$$J_4 = \frac{E_{k,nc} - E_{k,c}}{E_{k,nc}} \times 100\% \tag{14}$$

where u_{nc}, $\ddot{u}_{nc}$, $V_{b,nc}$, and $E_{k,nc}$ are respectively the maximum relative displacement, maximum absolute acceleration, maximum base shear and maximum kinetic energy of the uncontrolled buildings. The corresponding notations for controlled buildings are u_c, $\ddot{u}_c$, $V_{b,c}$, and $E_{k,c}$.

4. TMDI attached on SDOF main structure

The parameters of the TMDI are optimized considering different conditions of the main structure from very flexible (soft soil) to the rigid foundation (fixed base). The ranges for optimization of frequency tuning ratio and damping ratio of the TMDI are given in Table 5.

Knowing that a TMDI is consisting of physical mass m_t, damping c_t, stiffness k_t, and inerter mass ratio β_t. The m_t of TMDI can be calculated by assuming its ratio μ_t to the total mass of structure. In this study the objective is to minimize the transfer function of the roof displacement of the building. Therefore, the H_2-norm method and genetic algorithm (GA) are used to minimize the transfer function. The optimization process for the Tuned Mass Damper Inerter (TMDI) incorporating Soil-Structure Interaction (SSI) is depicted in Fig. 3, providing a comprehensive and systematic overview of the methodology. This intricately designed flowchart

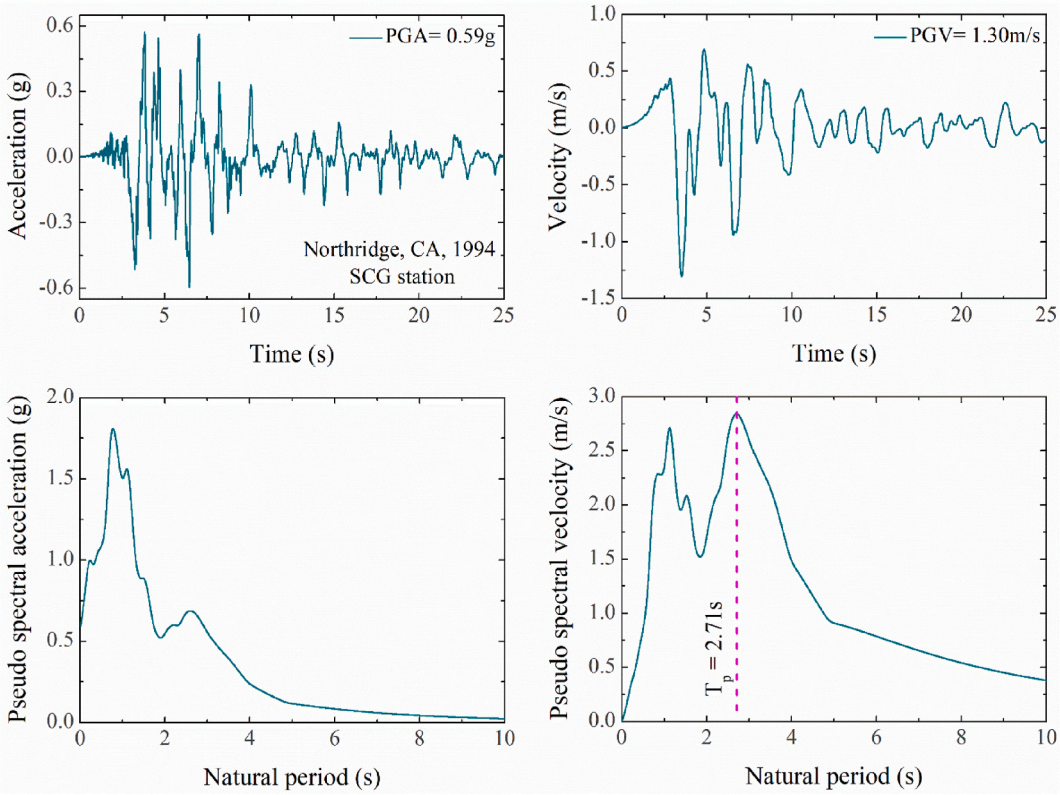

Fig. 14. Acceleration, velocity time histories and elastic response spectra (5 % damped) of the Northridge ground motion recorded. The pulse period is presented with the vertical dashed line.

outlines the step-by-step procedures employed to enhance the TMDI's performance in the context of dynamic soil-structure interactions. The journey begins with the incorporation of H2 control strategies, a sophisticated approach designed to optimize the TMDI's efficiency. This initial phase sets the foundation for achieving enhanced damping characteristics tailored to the specific dynamics of the structure and its interaction with the surrounding soil. As the process unfolds, the Genetic Algorithm (GA) takes center stage, introducing a powerful optimization tool to fine-tune the parameters of the TMDI. This genetic algorithm, inspired by the principles of natural selection, systematically explores the solution space to identify optimal configurations that maximize the system's performance under dynamic loads. The iterative interplay between H2 and GA, as illustrated in the flowchart, reflects a meticulous and adaptive optimization process. It highlights the dynamic nature of the TMDI's tuning, acknowledging the complex interdependencies between structural dynamics and soil interactions. This comprehensive approach, depicted in Fig. 3, serves as a roadmap for harnessing advanced control strategies to optimize the TMDI's effectiveness in real-world scenarios. The interweaving of H2 and GA techniques in the optimization process underscores a sophisticated and adaptive methodology, aiming to elevate the TMDI's performance in the face of diverse and dynamic structural challenges.

The SDOF model considered is the equivalent to the five story multi-degree of freedom (MDOF) presented by Salvi [75]. The frequency of the fixed base SDOF is 1.112 Hz, and three types of soils such as dense, medium, and soft are considered. The corresponding frequencies are 1.108 Hz, 1.100 Hz, and 1.017 Hz, respectively. Fig. 4 shows the variation of optimum parameters for different mass ratio of the TMDI and inerter (inertance).

The mass ratio (m_t) is increased up to 40 % of the total mass of the building, whereas the mass ratio of the inerter (β_t) is increased up to 100 %. The values are selected to show the pattern only, as it is known that there is practical restriction for large masses. It is observed that the optimum frequency ratio decreased by increasing the mass ratio. Oppositely the optimum damping ratio increased by increasing the mass ratio.

In order to depict a more comprehensive trend, the natural period of the SDOF system is systematically increased up to 4 s, reflecting the presence of numerous SDOF systems, each representing distinct periods. Figs. 5 and 6 show the displacement reduction (four cases are compared) of the SDOF system considering SSI and the period is increased up to 4 s. It is observed that for fixed base system the reduction pattern is consistent for most of the natural periods. In some cases where the response is amplified will be discussed in the next section. As much the flexibility in soil is increased the TMDI is less effective to mitigate the displacement response of rigid buildings. For example, in case of soft soil, the TMDI has no or less effect in reducing the displacement response of buildings with natural time periods below 0.6 s.

This indicates two facts, first that SSI creates spaced frequency where the TMDI is not able to effectively reduce the response and

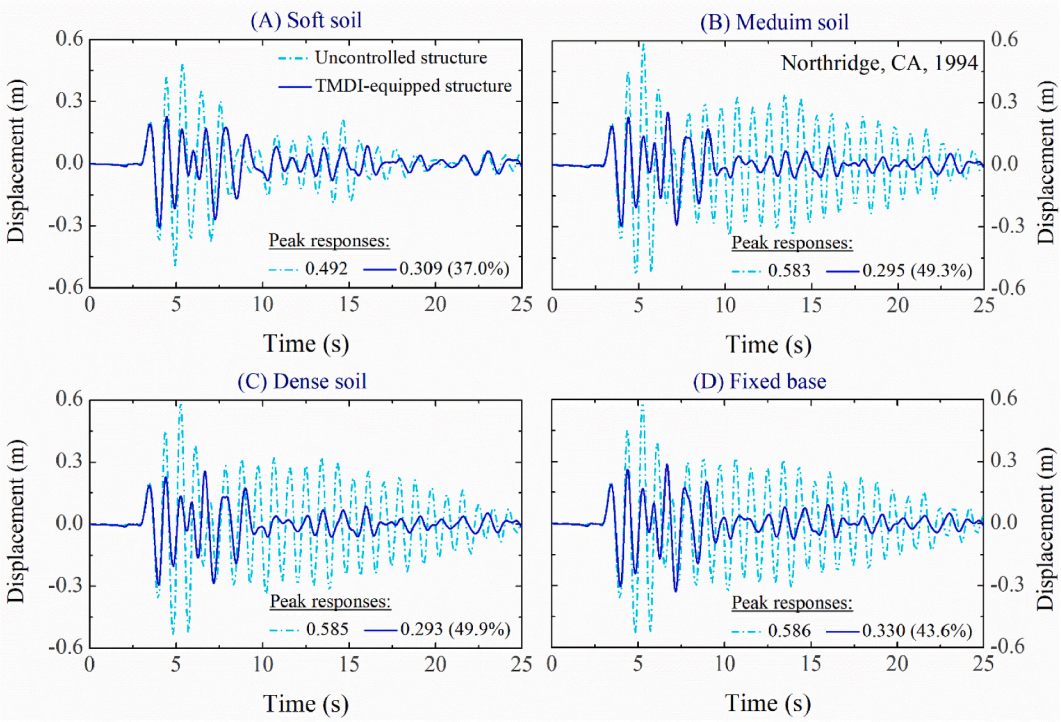

Fig. 15. Time variation of top floor displacement for the best response reduction in to low-rise-five-story building with and without controlled subjected to Northridge ground motion.

secondly, the overall performance of TMDI is higher for high-rise buildings (more flexible). Above 1 s period the response reduction is more consistent. Hence, the selection includes two additional examples, a five-story building with a fundamental frequency of 1.112 Hz and a forty-story building with a fundamental frequency of 0.261 Hz. These examples showcase more-realistic structures with multiple modes, and notably, the TMDI is not attached to the ground in these instances.

Figs. 7 and 8 show the reduction in maximum acceleration response in the SDOF systems. Largely, the TMDI's effectiveness in mitigating acceleration response is compromised as its parameters are optimized by minimizing the displacement transfer function. The pattern of acceleration response reduction is quite opposite to that of displacement response. As much the flexibility (natural period) is increased the effectiveness is reduced. It is commonly understood that acceleration response is higher in low-rise buildings when subjected to earthquake ground motions. Therefore, the effectiveness of TMDI in mitigating such high acceleration response is a positive sign. However, it is also highlighted the need for a multi-objective optimization method to significantly mitigate both the displacement and acceleration response. Generally, the TMDI is more effective in reducing large vibration, this is because the device capacity is higher to dissipate the energy. In addition, it is observed that the TMDI is less sensitive to soil conditions and acts robustly.

5. Effectiveness of TMDI on low-rise building

In this section, we present the effectiveness of the TMDI in mitigating the of a five-story low-rise building. The building's properties are detailed in Tables 1 and it is selected from existing literature for comparison with published results, ensuring the validity of our findings.

Fig. 9 validates the multi-modal frequencies of the selected building, both with and without considering the SSI. The results match those reported by Salvi et al. [75], confirming the accuracy of our study.

In this example we designed and installed the TMDI without grounding it (see Fig. 1), making it more realistic. Similar to the previous case, we optimize the parameters of the TMDI by minimizing the displacement transfer. The optimum parameters of the TMDI obtained using H_2 and genetic algorithm, are provided in Table 6, where the mean of the transfer function is minimized.

Figs. 10 and 11 demonstrate the transfer function of both displacement and acceleration response respectively. It is evident that the optimized TMDI has substantially reduced the transfer function for both displacement and acceleration response.

The transfer function of the acceleration response clearly indicates the presence of multi-mode contribution. In the controlled buildings' acceleration transfer function, two peaks of unequal height are evident, highlighting the necessity for a multi-objective optimization technique. Future studies should consider or develop such a technique to achieve a robust design of TMDI. To evaluate TMDI's effectiveness, pulse-like ground motions are selected in this study.

Fig. 12 shows the percentage reduction (J_i, %) in displacement, acceleration, and base shear for the buildings. The optimized TMDI proves to be significantly effective in reducing the buildings' response under the ground motions, particularly when the response is

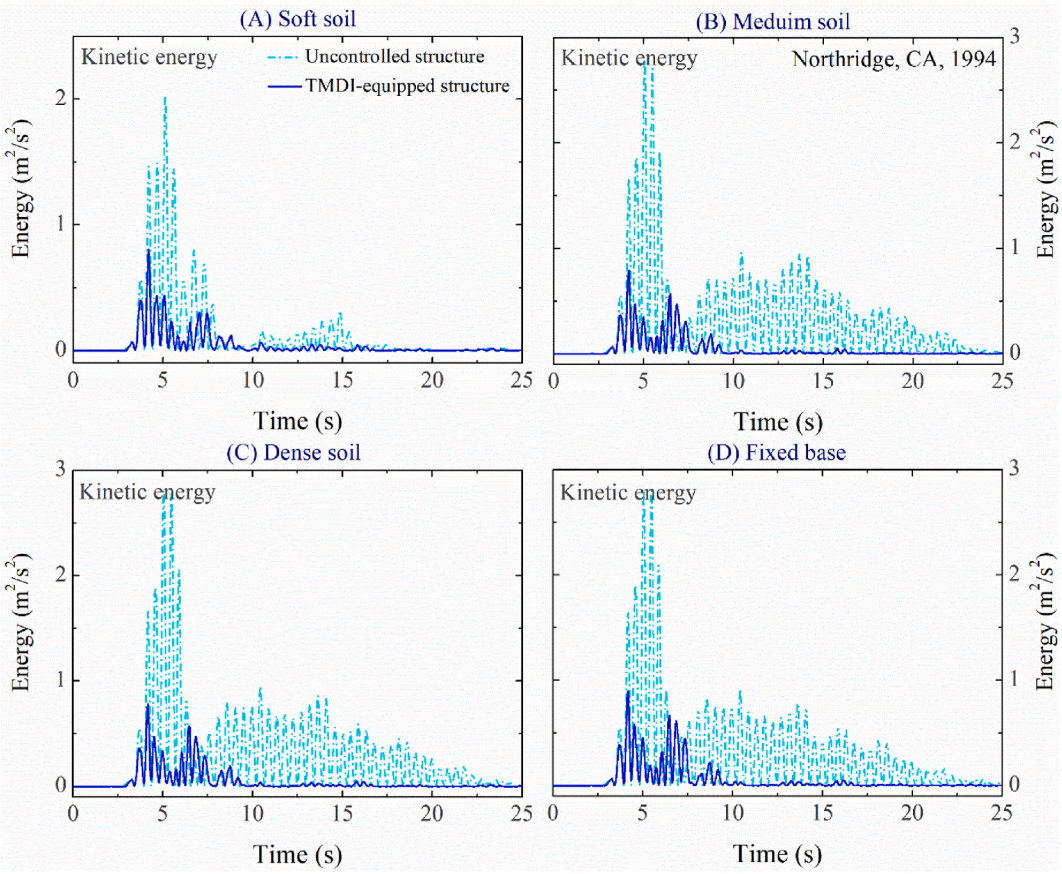

Fig. 16. Time variation of kinetic energy for the best response reduction in low-rise-five-story building with and without controlled subjected to Northridge ground motion.

large. Although there are cases where the TMDI amplifies the response, mainly, when considering soft soil conditions, it is not a major concern because the TMDI's ineffectiveness is observed only for buildings with low response levels. The optimized TMDI demonstrates higher effectiveness when the pulse period is close to the natural period of the buildings, which is known as the resonance condition.

In such cases, the TMDI efficiently mitigates the response. While the TMDI proves highly effective in mitigating structural response, it is crucial to recognize that its efficacy diminishes when the pulse period surpasses the natural period of the building, particularly evident in soft soil conditions. This nuanced understanding challenges the common assumption that a higher pulse period implies first-mode dominance. Instead, it underscores a reduced resonance between the structure and pulse period, ultimately leading to the diminished effectiveness of the TMDI. This revelation is paramount for optimizing the application of TMDI, paving the way for groundbreaking advancements in structural control under varying dynamic conditions. In order to conduct a thorough analysis of the data, specific box plots are created for each soil condition and fixed base building. These box plots are presented in Fig. 13, allowing for easy comparison to determine the effectiveness of the TMDI in each case.

The results from the box plots demonstrate that the TMDI is generally effective in reducing both displacement and acceleration response of the buildings, except when soft soil is considered. In those cases, the TMDI's effectiveness is limited in reducing displacement and acceleration response. Additionally, the TMDI has minimal impact on reducing the base shear of the buildings, as evident in J_3.

In order to show the conditions under which the TMDI can be effective or ineffective, two earthquake ground motions are selected. In the first case, we presented how the TMDI proves to be effective, while in the second case we showed its ineffectiveness.

Fig. 14 meticulously presents the distinctive characteristics of the Northridge ground motion. Notably, the figure illustrates a prominent pulse period (Tp = 2.71s); however, an additional pulse period around 1s is discernible. This dual-pulse feature suggests the potential for resonance conditions, creating a scenario where the TMDI is expected to be highly effective, as depicted in Fig. 15. Fig. 15 displays the time history of the displacement response for a fixed-base building and buildings accounting for various soil conditions. Notably, in the presence of soft soil, the effectiveness of the Tuned Mass Damper with Inerter (TMDI) is notably reduced when compared to the fixed base, as well as medium and dense soil conditions.

The distinctive behavior observed in the soft soil scenario stems from a noteworthy phenomenon: the height of the second peak in the controlled building's response surpasses that of the first peak. This unique dynamic results in a lower stroke for the Tuned Mass

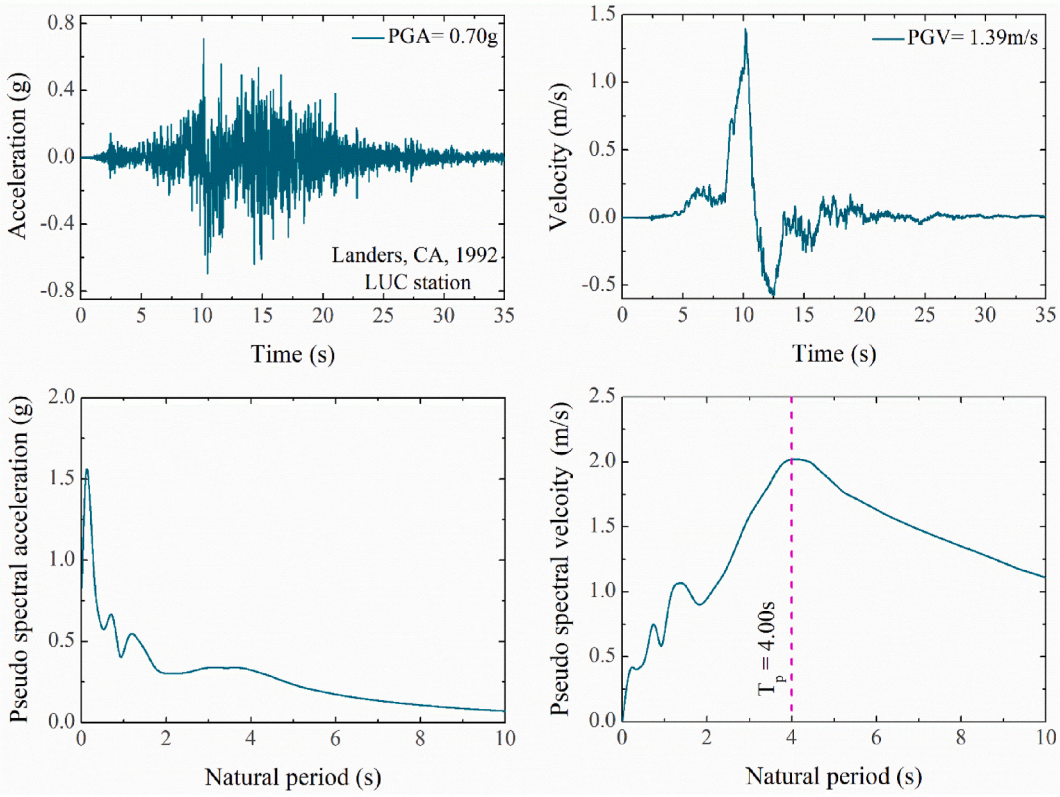

Fig. 17. Acceleration, velocity time histories and elastic response spectra (5 % damped) of the Landers ground motion. The pulse period is presented with the vertical dashed line.

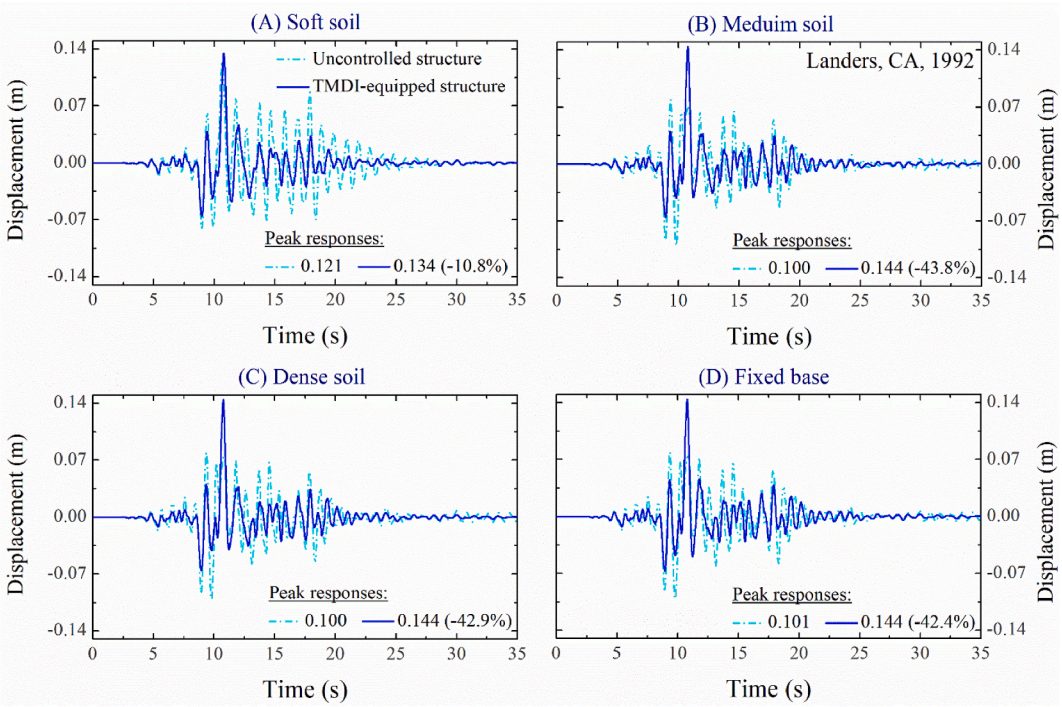

Fig. 18. Time variation of top floor displacement for the worst response reduction in low-rise-five-story building with and without controlled subjected to Landers ground motion.

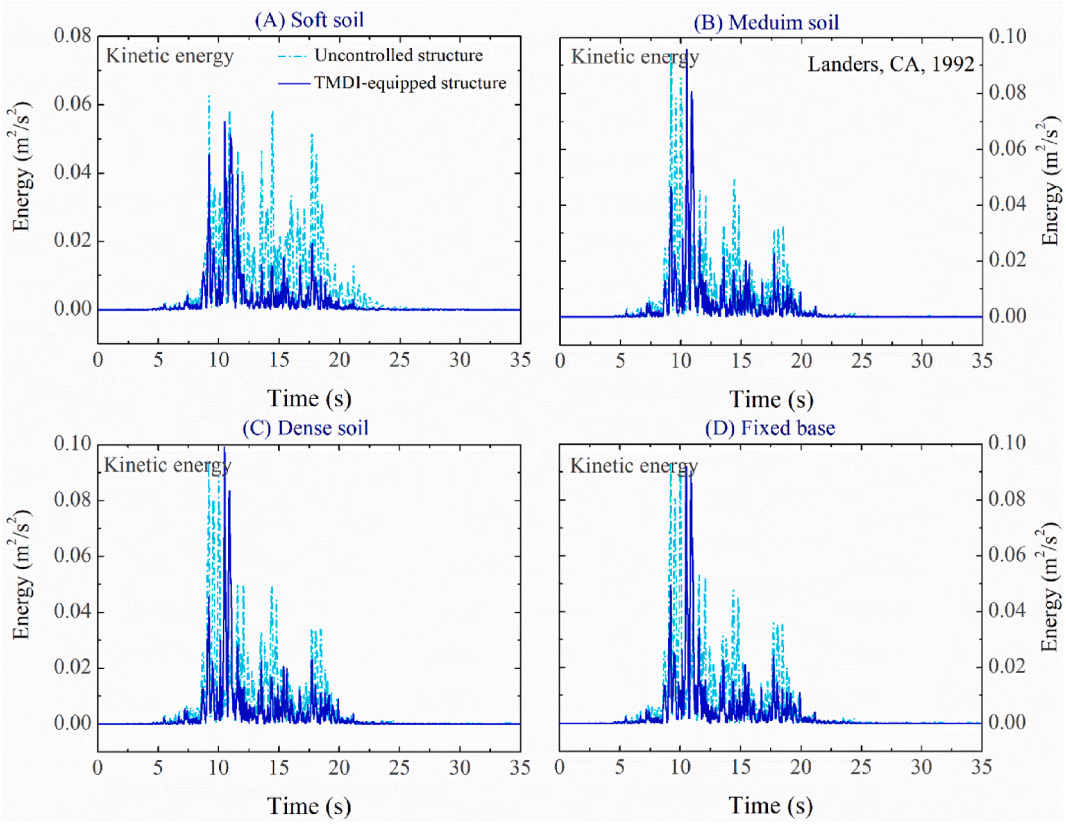

Fig. 19. Time variation of kinetic energy per unit mass for the worst response reduction in low-rise-five-story building with and without controlled subjected to Landers ground motion.

Table 7
Optimum TMDI parameters for high-rise forty-story building.

Variables	Soft soil	Medium soil	Dense soil	Fixed base
υ_t	1.122	1.122	1.122	1.122
ξ_t	0.141	0.141	0.141	0.141
μ_t	0.01	0.01	0.01	0.01
β_t	0.4	0.4	0.4	0.4
m_t (t)	392	392	392	392
b_t (t)	15680	15680	15680	15680
k_t (MN/m)	19.014	19.114	19.214	19.314
c_t (MN s/m)	8.744	8.764	8.772	8.763

Damper with Inerter (TMDI). Consequently, the TMDI exhibits a more modest reduction in response, approximately around 37 %, compared to other scenarios where its effectiveness is notably higher. This nuanced understanding sheds light on the critical influence of soil conditions on the TMDI's performance, paving the way for more refined and effective structural control strategies.

Fig. 16 provides a temporal depiction of the kinetic energy for both the uncontrolled and controlled buildings. The discernible trend indicates that the Tuned Mass Damper with Inerter (TMDI) significantly dissipates energy, reaffirming its reduced effectiveness in the context of soft soil conditions. Notably, around the first peak, the TMDI exhibits lower energy dissipation compared to other scenarios, contributing to its lesser effectiveness in mitigating the response of buildings with soft soil conditions. Despite this, the TMDI remains notably effective in reducing overall response.

To further underscore this observation, an earthquake ground motion with a pulse period exceeding the natural period of the building is selected in Fig. 17. Analyzing the Landers earthquake ground motion, it becomes evident that the pulse period is considerably higher than the natural period of the five-story building, with other peaks closer to the building's period significantly low, indicating the absence of a resonance condition. As a consequence, the TMDI proves ineffective in mitigating the response, as illustrated in Fig. 18. Fig. 19 further supports this by showcasing that the energy dissipated by the TMDI is not substantial. In all presented cases, the TMDI not only fails to reduce but even amplifies the response. This nuanced analysis underlines the varying effectiveness of the TMDI in different seismic scenarios, providing valuable insights for tailored structural control strategies.

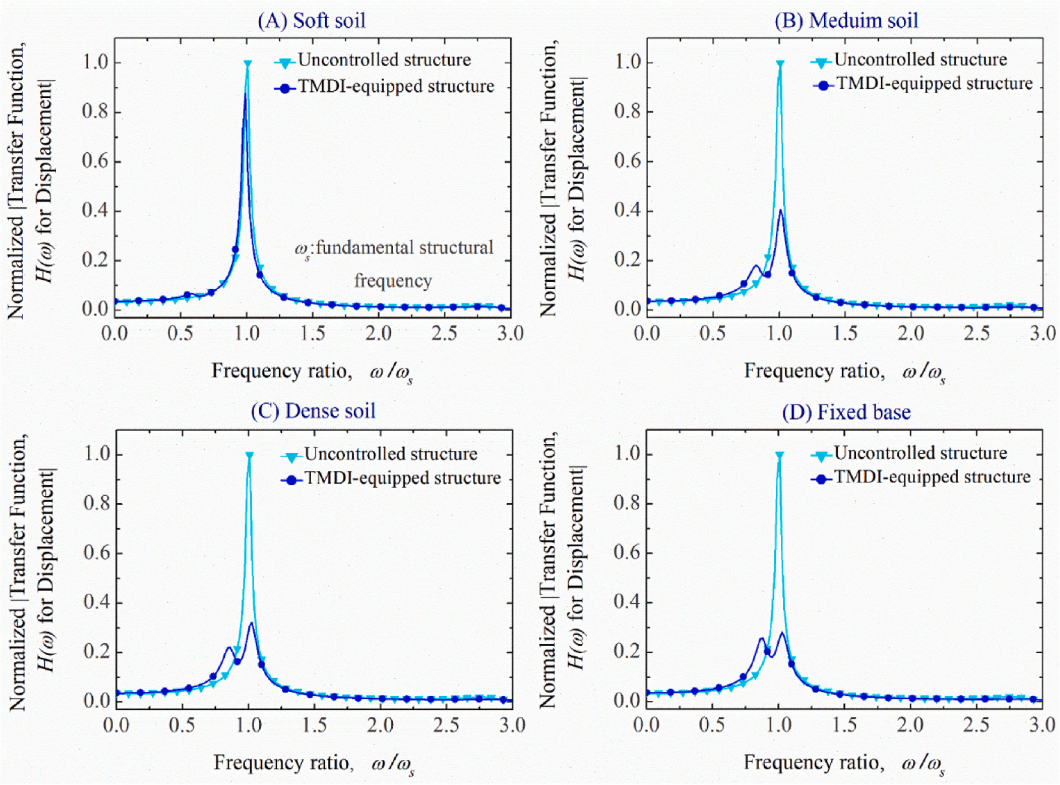

Fig. 20. Frequency domain transfer function curves $[H(\omega)]$ of the displacement for forty-story uncontrolled building and controlled with TMDI, considering different variable soil properties.

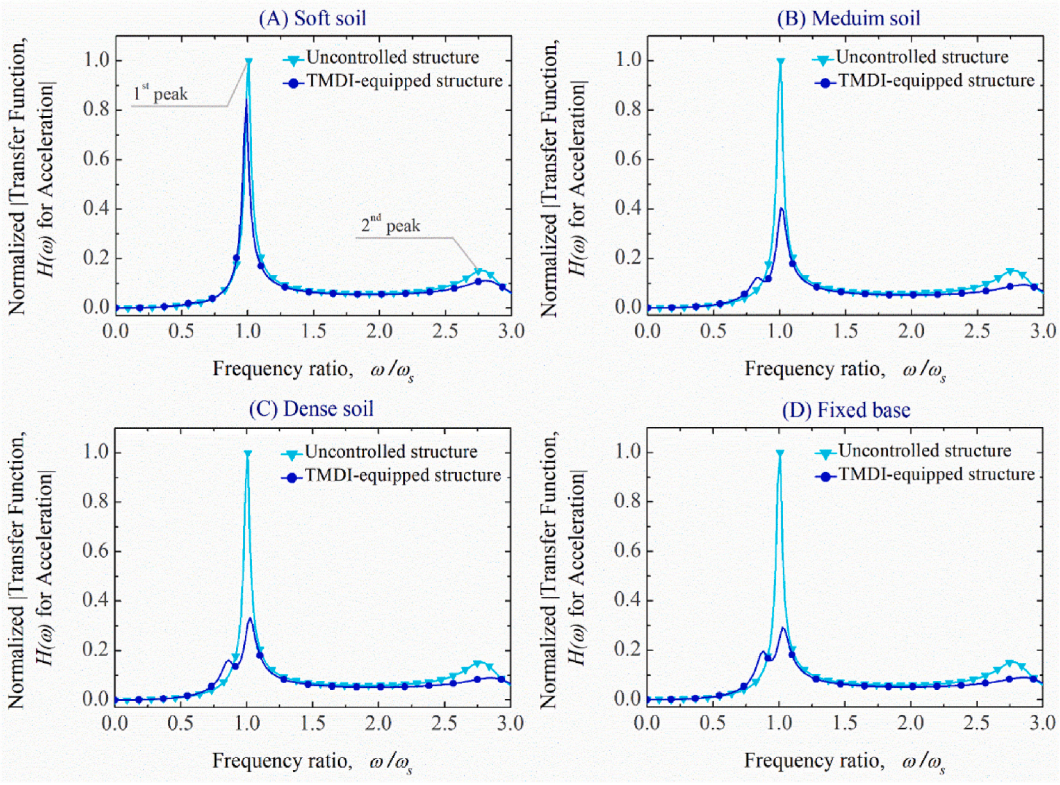

Fig. 21. Frequency domain transfer function curves $[H(\omega)]$ of the acceleration for forty-story uncontrolled building and controlled with TMDI, at different variable soil properties.

6. Effectiveness of TMDI installed on high-rise buildings

In this section, we introduce a forty-story building to represent a high-rise structure. The level of flexibility at its base is increased by considering the SSI effect. The performance of the fixed base building is compared to buildings with flexible bases when subjected to pulse-like ground motions. The detailed properties of the selected building are provided in Table 2, and the model accuracy is validated in Fig. 8, where the frequencies match those reported by Salvi et al. [75].

The optimum parameters of the TMDI for this high-rise building are listed in Table 7, following the same design concept as explained earlier for SDOF and low-rise buildings. Figs. 20 and 21 show the normalized transfer function for displacement and acceleration response, respectively. It is observed that in cases of fixed base building and considering a dense soil condition, the TMDI significantly reduces both the transfer functions for the displacement and acceleration response.

In the case of soft soil, the effectiveness of the TMDI is not significant. For medium soil, the TMDI performs better than the soft soil case but remains less effective than the fixed base and dense soil condition. It is important to note the in this example, the placement of the inerter is not optimized.

Fig. 22 shows the variation or response reduction considering the uncontrolled response and normalized periods. It is observed that most of the displacement response are below 1 m, and the corresponding acceleration is below 1g (where $g = 9.81$ m/s^2 is the gravitational acceleration). Interestingly, the TMDI proves effective in reducing the displacement response for all cases considered. However, ground motions tend to cause resonance around the second natural period of the building (see Fig. 22d). When the pulse period is greater than the natural period of the building, the effectiveness of the TMDI is not significant, and it may even amplify the response. However, when the pulse period coincided with the second or third natural period of the building, the TMDI remains effective.

It is important to note that the working principle of the TMDI is not limited to controlling only a single mode as in a traditional tuned mass damper (TMD). Instead, the TMDI's capacity is higher and can effectively mitigate the response across multiple modes.

Regarding the acceleration response, the TMDI can amplify the response when considering soft soil conditions. However, it remains significantly effective in mitigating the acceleration response for cases of fixed base and dense soil conditions (see Fig. 23).

In all considered cases, the TMDI is not effective in reducing the base shear of the buildings. This is because, in high-rise buildings, the maximum acceleration is not necessarily at the top floor during earthquakes. The multi-mode contribution of the building leads to this behavior. Therefore, a practical future solution would be to develop control strategies that effectively target and control multiple modes simultaneously.

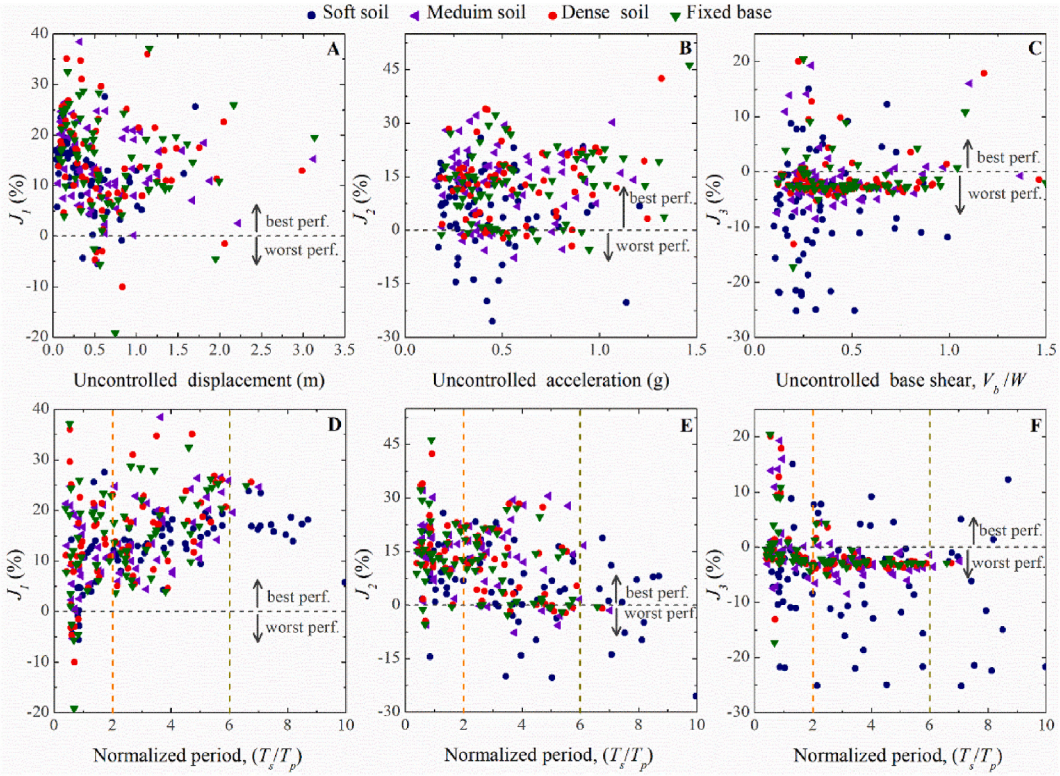

Fig. 22. Variation of J_i with respect to the variation of (A) uncontrolled peak displacement, (B) uncontrolled peak acceleration, (C) uncontrolled normalized base shear, (D, E and F) normalized period (T_s/T_p).The results correspond to high-rise-forty-story building.

7. Conclusions

In this comprehensive study, we have conducted a thorough assessment of the effectiveness of the Tuned Mass Damper Inerter (TMDI) in mitigating building responses, with a keen consideration of Soil-Structure Interaction (SSI). Our investigation encompasses three distinct models: Single Degree of Freedom (SDOF), low-rise Multi-Degree of Freedom (MDOF), and high-rise MDOF. Notably, we vary the natural period of the SDOF model to discern the TMDI's effectiveness across a spectrum of scenarios. Through pulse-like ground motions and a meticulous analysis in both frequency and time domains, our study yields the following key conclusions.

- The optimized TMDI emerges as significantly effective in attenuating the displacement response of buildings, particularly when the pulse period aligns closely with the natural period of the structures.
- While the proposed optimization method demonstrates substantial effectiveness in reducing displacement responses, its impact on mitigating acceleration responses is limited, highlighting the need for multi-objective optimization techniques.
- Overall, the TMDI exhibits limited effectiveness in mitigating base shear responses, underscoring the necessity for adopting multi-mode response control strategies for buildings.
- A notable pattern emerges, showcasing the TMDI's effectiveness when structures experience substantial responses, providing a safety net for buildings under worst-case conditions.
- Our analysis of the TMDI has unveiled critical insights into its performance across varied seismic scenarios. Notably, its effectiveness is affirmed by substantial energy dissipation in soft soil conditions. However, a closer examination reveals nuanced dynamics: around the first peak, lower energy dissipation reduces its efficacy in mitigating responses under soft soil conditions. Furthermore, introducing a seismic condition with a pulse period exceeding the natural period of the building emphasizes a crucial lesson. The subsequent analysis underscores the TMDI's ineffectiveness in the absence of resonance conditions, leading to response amplification rather than reduction. This nuanced understanding underscores the imperative for tailored structural control strategies, recognizing the TMDI's varying effectiveness in different seismic contexts.

These conclusive findings offer valuable insights into the application and optimization of the TMDI, enriching our understanding of its potential to enhance seismic performance across diverse scenarios. This study underscores the intricate interplay between TMDI, building dynamics, and soil interactions, contributing to the broader discourse on resilient and adaptive structural control strategies.

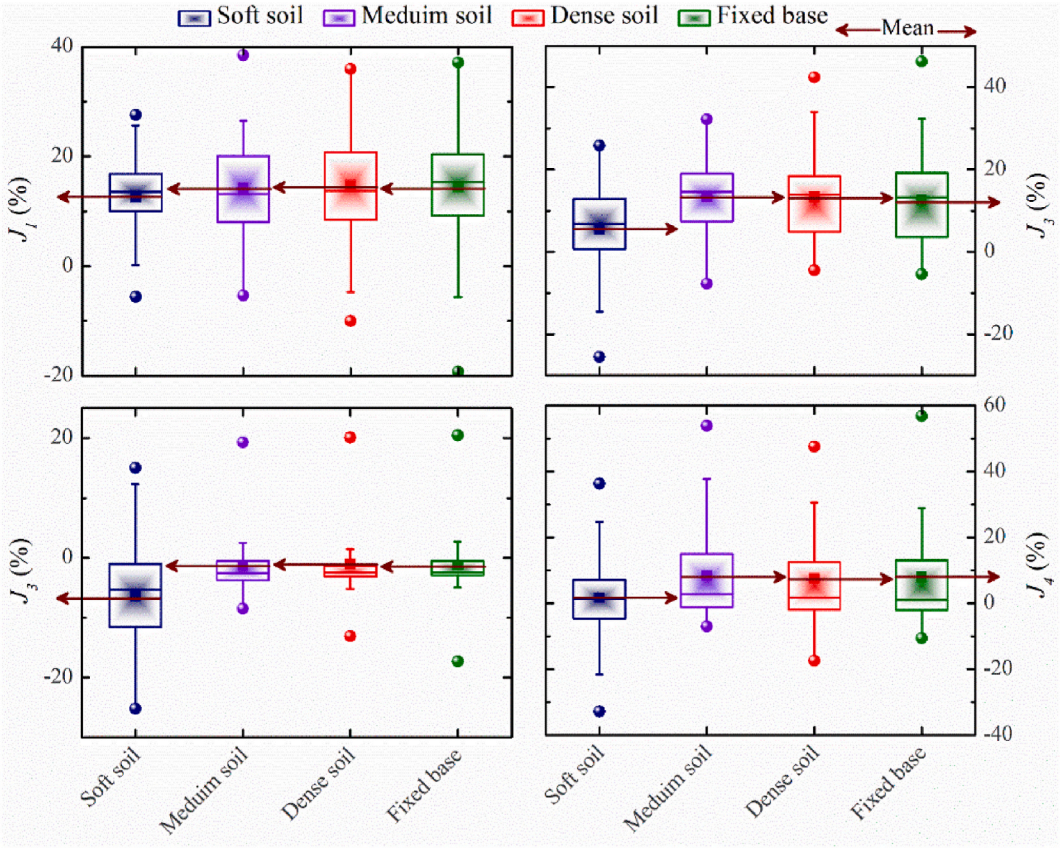

Fig. 23. Box plots of the percentage response reduction data J_1, J_2, J_3 and J_4 to forty-story building with different soil properties and under pulse-like ground motions records.

CRediT authorship contribution statement

Said Elias: Conceptualization, Investigation, Methodology, Software, Supervision, Validation, Writing – original draft, Writing – review & editing. **Salah Djerouni:** Formal analysis, Investigation, Methodology, Software, Validation, Writing – original draft.

Declaration of competing interest

The authors declare that they have no known competing financial interests or personal relationships that could have appeared to influence the work reported in this paper.

Data availability

Data will be made available on request.

Acknowledgement

The authors express their gratitude to the Ministry of Higher Education and Scientific Research in Algeria for extending a fellowship to the second author under the National Exceptional Program (ENP). The funds for second author during his stay at the University of Iceland provided by the Earthquake Engineering Research Centre are aknowledged. Furthermore, the appreciation is extended to the University of Twente and Leibniz University Hannover for their support in providing research equipment to the first author. These collaborative efforts and support systems have significantly contributed to the successful execution of this research endeavor.

Appendix

Table A1
List and information of the considered near-fault pulse-like ground motions in this study [71].

Earthquake	Date	Station	Comp	*M*	R_{jb} (km)	*T* (sec)	*PGA* (g)	*PGV* (cm/s)	*Vs30* (cm/s)
Chi-Chi, Taiwan	20-Sep-99	TCU103	SN	7.6	6.1	7.2152	0.1323	62.5	494.1
Izmit, Tukey	17-Aug-99	ARC	SN	7.51	10.56	6.	0.1331	44.3	523
Chi-Chi, Taiwan	20-Sep-99	TCU036	SN	7.6	19.84	5.0845	0.1345	62.3	272.6
Chi-Chi, Taiwan	20-Sep-99	TCU046	SN	7.6	16.74	6.7891	0.1394	44.33	465.55
Chi-Chi, Taiwan	20-Sep-99	TCU038	SN	7.6	25.44	5.9202	0.1398	50.9	272.6
Chi-Chi, Taiwan	20-Sep-99	TCU040	SN	7.6	22.08	5.6132	0.1452	53.2	362.03
Parkfield, CA, USA	28-Sep-04	Parkfield fault zone 9	SN	6	1.25	1.0056	0.1578	26.1	438
Chi-Chi, Taiwan	20-Sep-99	TCU054	SN	7.6	5.3	6.6866	0.1689	61.2	460.69
Parkfield, CA, USA	28-Sep-04	Parkfield Cholame 4A	SN	6	4.69	0.8571	0.1856	22.16	339
Chi-Chi, Taiwan	20-Sep-99	TCU128	SN	7.6	13.15	4.712	0.1874	78.3	599.64
Chi-Chi, Taiwan	20-Sep-99	TCU042	SN	7.6	26.32	7.2152	0.2089	47.5	272.6
Landers, CA, USA	28-Jun-92	Yermo Fire	SN	7.28	23.62	6.841	0.2218	53.2	353.63
Chi-Chi, Taiwan	20-Sep-99	TCU053	SN	7.6	5.97	9.7819	0.2247	41.9	454.55
Irpinia, Italy-01	23-Nov-80	Sturno	SN	6.9	6.78	2.5442	0.2313	41.5	1000
Whittier Infrrows, USA	10-Oct-87	DOW	SN	5.99	14.95	0.7305	0.2341	30.4	271.9
Morgan Hill, CA, USA	24-Apr-84	Gilroy Array # 6	SN	6.19	9.85	1.1532	0.2430	35.4	663.31
Chi-Chi, Taiwan	20-Sep-99	TCU082	SN	7.6	5.18	6.8932	0.2477	56.4	472.81
Whittier Infrrows, USA	10-Oct-87	LB Orange Eve	SN	5.99	19.8	0.7086	0.2554	32.9	270.19
Izmit, Tukey	17-Aug-99	GBZ	SN	7.51	7.57	4.6057	0.2633	41.4	792
Northridge, CA, U.S.A.	17-Jan-94	LA Wadsworth VA hospital North	SN	6.7	14.55	2.27	0.2735	32.4	392.24
Chi-Chi, Taiwan	20-Sep-99	TCU049	SN	7.6	3.78	9.2746	0.2810	45.1	487.27
Superstition Hills, CA, USA	24-Nov-87	ELC	SN	6.54	18.2	1.96	0.2973	52	192.05
Chi-Chi, Taiwan	20-Sep-99	TCU076	SN	7.6	2.76	3.3714	0.3004	63.7	614.98
Imperial Valley, USA	15-Oct-79	Agrarias	SN	6.53	0	1.8766	0.3115	54.4	274.5
Morgan Hill, CA, USA	24-Apr-84	HAL	SN	6.19	3.45	0.8314	0.3141	39.7	281.61
Chi-Chi, Taiwan	20-Sep-99	TCU075	SN	7.6	0.91	4.4338	0.3331	88.3	573.02
Parkfield, CA, USA	28-Sep-04	Parkfield Cholame 2 east	SN	6	2.5	0.82	0.3365	23.66	376
Palm Springs, CA, USA	08-Jul-86	DSP	SN	6.06	0.99	1.28	0.3427	29.7	345.42
Imperial Valley, USA	15-Oct-79	Aeroporto Mexicalli	SN	6.53	0	1.5995	0.3573	44.3	274.5
Loma Prieta, CA, USA	17-Oct-89	STG	SN	6.93	7.58	1.5516	0.3653	57.2	370.79
Imperial Valley, USA	15-Oct-79	EC Meloland Overpass FF	SN	6.53	0.07	2.8518	0.3780	115	186.21
L'Aquila, Italy	06-Apr-09	AQK	SN	6.3	0	1.5754	0.3799	46.7	580
Parkfield, CA, USA	28-Sep-04	Parkfield fault zone 12	SN	6	0.94	1.0056	0.3821	57.5	339
Loma Prieta, CA, USA	17-Oct-89	Gilroy Array #2	SN	6.93	10.38	1.46	0.4062	45.7	270.84
Superstition Hills, USA	24-Nov-87	PTS	SN	6.54	0.95	1.8624	0.4186	106.8	348.69
Northridge, CA, USA	17-Jan-94	NWS	SN	6.7	2.11	2.025	0.4257	87.75	285.93
Parkfield, CA, USA	28-Sep-04	Parkfield Cholame 3 west	SN	6	2.5	0.6822	0.4416	45	339
Coyote lake, CA, USA	08-Jun-79	GA6	SN	5.74	0.42	0.8189	0.4519	51.5	663.61
Parkfield, CA, USA	28-Sep-04	Parkfield Cholame 2 west	SN	6	1.88	0.8703	0.4605	49.98	185
Chi-Chi, Taiwan aftershock	20-Sep-99	CHY080	SN	6.2	21.34	1.1017	0.4659	70.31	553.4
Parkfield, CA, USA	28-Sep-04	Parkfield Cholame 1 east	SN	6	1.88	1.0606	0.4713	52.82	339
Parkfield, CA, USA	27-Jun-66	CO2	SN	6.19	6.27	1.68	0.4759	75.1	184.8
Erzincan, Turkey	13-Mar-92	ERZ	SN	6.69	0	2.2355	0.4834	95.4	274.5
Parkfield, CA, USA	28-Sep-04	Parkfield fault zone 1	SN	6	0	1.1186	0.4977	64.15	339
Northridge, CA, USA	17-Jan-94	JFA	SN	6.7	0	2.6631	0.5164	67.42	373.07
Northridge, CA, USA	17-Jan-94	JFA generator	SN	6.7	0	2.6631	0.5165	67.4	525.79
Chi-Chi, Taiwan aftershock	20-Sep-99	TCU076	SN	6.2	13.04	0.7141	0.5238	58.9	614.98
Northridge, CA, USA	17-Jan-94	LA Dam (LDW)	SN	6.7	0	1.2926	0.5700	75.21	628.99

(*continued on next page*)

Table A1 (*continued*)

Earthquake	Date	Station	Comp	*M*	R_{jb} (km)	*T* (sec)	*PGA* (g)	*PGV* (cm/s)	*Vs30* (cm/s)
Parkfield, CA, USA	28-Sep-04	Parkfield Cholame 4 west	SN	6	3.44	0.5815	0.5728	38.37	438
Northridge, CA, USA	17-Jan-94	SCG	SN	6.7	0	2.71	0.5943	130.3	251.24
Gazli, USSR	17-Mar-76	KAR	SN	6.8	3.92	4.1	0.6080	65.32	659.6
Kobe, Japan	19-Jan-95	Takarazuka	SN	6.9	0	1.2163	0.6452	72.6	312
Loma Prieta, CA, USA	17-Oct-89	LGP	SN	6.93	0	1.57	0.6461	103.2	477.65
Palm Springs, CA, USA	08-Jul-86	NPS	SN	6.06	0	1.0934	0.6659	73.64	345.42
Landers, CA, USA	28-Jun-92	LUC	SN	7.28	2.19	4.0778	0.7088	140	684.94
Northridge, CA, U.S.A.	17-Jan-94	Sylmar Olive View Medical FF	S.N.	6.7	1.74	2.4123	0.7326	122.7	44054
Chi-Chi, Taiwan	20-Sep-99	TCU065	SN	7.6	0.59	4.3009	0.8218	127.8	305.85
Northridge, CA, USA	17-Jan-94	SCH	SN	6.7	0	2.9177	0.8387	116.6	370.52
San Salvador	10-Oct-86	Geotech Investigation center	SN	5.8	2.14	0.6668	0.8446	62.3	545
Tabas, Iran	16-Sep-78	TAB	SP	7.11	1.79	4.712	0.8472	117.7	766.77
Chi-Chi, Taiwan	20-Sep-99	TCU129	SN	7.6	1.84	5.69	0.9816	71.47	664.43
San FerInfndo, USA	09-Feb-71	PCD	SN	6.61	0	1.1532	1.4345	116.5	2016.1

References

[1] S. Elias, V. Matsagar, Wind response control of 76-storey benchmark building with distributed multiple tuned mass dampers, J. Wind Eng. 11 (2) (2014) 37–49.
[2] S. Djerouni, S. Elias, M. Abdeddaim, R. Rupakhety, Optimal design and performance assessment of multiple tuned mass damper inerters to mitigate seismic pounding of adjacent buildings, J. Build. Eng. 48 (2022) 103994.
[3] S. Elias, Seismic energy assessment of buildings with tuned vibration absorbers, Shock Vib. 2018 (2018) 1–10.
[4] S. Elias, V. Matsagar, T.K. Datta, Distributed tuned mass dampers for multi-mode control of benchmark building under seismic excitations, J. Earthq. Eng. 23 (7) (2019) 1137–1172.
[5] D. Caicedo, L. Lara-Valencia, J. Blandon, C. Graciano, Seismic response of high-rise buildings through metaheuristic-based optimization using tuned mass dampers and tuned mass dampers inerter, J. Build. Eng. 34 (2021) 101927.
[6] L. Wang, W. Shi, Y. Zhou, Adaptive-passive tuned mass damper for structural aseismic protection including soil–structure interaction, Soil Dynam. Earthq. Eng. 158 (2022) 107298.
[7] L. Wang, S. Nagarajaiah, W. Shi, Y. Zhou, Semi-active control of walking-induced vibrations in bridges using adaptive tuned mass damper considering human-structure-interaction, Eng. Struct. 244 (2021) 112743.
[8] Y. Wang, L. Wang, W. Shi, Two-dimensional air spring based semi-active TMD for vertical and lateral walking and wind-induced vibration control, Struct. Eng. Mech. 80 (4) (2021) 377–390.
[9] O. Araz, V. Kahya, Series tuned mass dampers in vibration control of continuous railway bridges. Structural Engineering and Mechanics, An Int'l Journal 73 (2) (2020) 133–141.
[10] O. Araz, V. Kahya, Optimization of multiple tuned mass dampers for a two-span continuous railway bridge via differential evolution algorithm, Structures 39 (2022, May) 29–38. Elsevier.
[11] C. Li, Optimum multiple tuned mass dampers for structures under the ground acceleration based on DDMF and ADMF, Earthq. Eng. Struct. Dynam. 31 (4) (2002) 897–919.
[12] L. Cao, C. Li, Tuned tandem mass dampers-inerters with broadband high effectiveness for structures under white noise base excitations, Struct. Control Health Monit. 26 (4) (2019) e2319.
[13] O. Araz, T. Cakir, K.F. Ozturk, Effect of earthquake frequency content on seismic-induced vibration control of structures equipped with tuned mass damper, J. Braz. Soc. Mech. Sci. Eng. 44 (12) (2022) 584.
[14] S. Djerouni, A. Ounis, S. Elias, M. Abdeddaim, R. Rupakhety, Optimization and performance assessment of tuned mass damper inerter systems for control of buildings subjected to pulse-like ground motions, Structures 38 (2022, April) 139–156. Elsevier.
[15] C. Li, Performance of multiple tuned mass dampers for attenuating undesirable oscillations of structures under the ground acceleration, Earthq. Eng. Struct. Dynam. 29 (9) (2000) 1405–1421.
[16] A.Y. Leung, H. Zhang, C.C. Cheng, Y.Y. Lee, Particle swarm optimization of TMD by non-stationary base excitation during earthquake, Earthq. Eng. Struct. Dynam. 37 (9) (2008) 1223–1246.
[17] T. Asami, O. Nishihara, A.M. Baz, Analytical solutions to H∞ and H 2 optimization of dynamic vibration absorbers attached to damped linear systems, J. Vib. Acoust. 124 (2) (2002) 284–295.
[18] Y. Fujino, M. Abé, Design formulas for tuned mass dampers based on a perturbation technique, Earthq. Eng. Struct. Dynam. 22 (10) (1993) 833–854.
[19] C. Li, B. Zhu, Estimating double tuned mass dampers for structures under ground acceleration using a novel optimum criterion, J. Sound Vib. 298 (1–2) (2006) 280–297.
[20] L. Cao, C. Li, A high performance hybrid passive base-isolated system, Struct. Control Health Monit. 29 (3) (2022) e2887.
[21] C. Li, K. Chang, L. Cao, Y. Huang, Performance of a nonlinear hybrid base isolation system under the ground motions, Soil Dynam. Earthq. Eng. 143 (2021) 106589.
[22] S.V. Bakre, R.S. Jangid, Optimum parameters of tuned mass damper for damped main system, Struct. Control Health Monit.: The Official Journal of the International Association for Structural Control and Monitoring and of the European Association for the Control of Structures 14 (3) (2007) 448–470.
[23] O. Araz, Optimization of three-element tuned mass damper based on minimization of the acceleration transfer function for seismically excited structures, J. Braz. Soc. Mech. Sci. Eng. 44 (10) (2022) 459.
[24] A.Y.T. Leung, H. Zhang, Particle swarm optimization of tuned mass dampers, Eng. Struct. 31 (3) (2009) 715–728.
[25] B. Brown, T. Singh, Minimax design of vibration absorbers for linear damped systems, J. Sound Vib. 330 (11) (2011) 2437–2448.
[26] H.Y. Zhang, L.J. Zhang, Tuned mass damper system of high-rise intake towers optimized by improved harmony search algorithm, Eng. Struct. 138 (2017) 270–282.
[27] A.S. Joshi, R.S. Jangid, Optimum parameters of multiple tuned mass dampers for base-excited damped systems, J. Sound Vib. 202 (5) (1997) 657–667.
[28] F. Sadek, B. Mohraz, A.W. Taylor, R.M. Chung, A method of estimating the parameters of tuned mass dampers for seismic applications, Earthq. Eng. Struct. Dynam. 26 (6) (1997) 617–635.
[29] M.N. Hadi, Y. Arfiadi, Optimum design of absorber for MDOF structures, J. Struct. Eng. 124 (11) (1998) 1272–1280.

[30] S. Elias, V. Matsagar, Research developments in vibration control of structures using passive tuned mass dampers, Annu. Rev. Control 44 (2017) 129–156.
[31] G. Bekdaş, S.M. Nigdeli, X.S. Yang, A novel bat algorithm based optimum tuning of mass dampers for improving the seismic safety of structures, Eng. Struct. 159 (2018) 89–98.
[32] M. Yucel, G. Bekdaş, S.M. Nigdeli, S. Sevgen, Estimation of optimum tuned mass damper parameters via machine learning, J. Build. Eng. 26 (2019) 100847.
[33] O. Araz, V. Kahya, Design of series tuned mass dampers for seismic control of structures using simulated annealing algorithm, Arch. Appl. Mech. 91 (2021) 4343–4359.
[34] M.C. Smith, Synthesis of mechanical networks: the inerter, IEEE Trans. Automat. Control 47 (10) (2002) 1648–1662.
[35] L. Marian, A. Giaralis, The tuned mass-damper-inerter for harmonic vibrations suppression, attached mass reduction, and energy harvesting, Smart Struct. Syst. 19 (6) (2017) 665–678.
[36] L. Marian, A. Giaralis, Optimal design of a novel tuned mass-damper–inerter (TMDI) passive vibration control configuration for stochastically support-excited structural systems, Probabilist. Eng. Mech. 38 (2014) 156–164.
[37] A.A. Taflanidis, A. Giaralis, D. Patsialis, Multi-objective optimal design of inerter-based vibration absorbers for earthquake protection of multi-storey building structures, J. Franklin Inst. 356 (14) (2019) 7754–7784.
[38] F. Petrini, A. Giaralis, Z. Wang, Optimal tuned mass-damper-inerter (TMDI) design in wind-excited tall buildings for occupants' comfort serviceability performance and energy harvesting, Eng. Struct. 204 (2020) 109904.
[39] L. Cao, C. Li, X. Chen, Performance of multiple tuned mass dampers-inerters for structures under harmonic ground acceleration, Smart Structures and Systems, An International Journal 26 (1) (2020) 49–61.
[40] C. Li, W. Qu, Optimum properties of multiple tuned mass dampers for reduction of translational and torsional response of structures subject to ground acceleration, Eng. Struct. 28 (4) (2006) 472–494.
[41] S. Djerouni, M. Abdeddaim, S. Elias, R. Rupakhety, Optimum double mass tuned damper inerter for control of structure subjected to ground motions, J. Build. Eng. 44 (2021) 103259.
[42] X. Shi, S. Zhu, A comparative study of vibration isolation performance using negative stiffness and inerter dampers, J. Franklin Inst. 356 (2019) 7922–7946, https://doi.org/10.1016/j.jfranklin.2019.02.040.
[43] M. Wang, F.F. Sun, S. Nagarajaiah, Simplified optimal design of MDOF structures with negative stiffness amplifying dampers based on effective damping, Struct. Des. Tall Special Build. 28 (2019) 1–26, https://doi.org/10.1002/tal.1664.
[44] M. Wang, F.F. Sun, J.Q. Yang, S. Nagarajaiah, Seismic protection of SDOF systems with a negative stiffness amplifying damper, Eng. Struct. 190 (2019) 128–141, https://doi.org/10.1016/j.engstruct.2019.03.110.
[45] H. Wang, H. Gao, J. Li, et al., Optimum design and performance evaluation of the tuned inerter-negative-stiffness damper for seismic protection of single-degree-of-freedom structures, Int. J. Mech. Sci. 212 (2021) 106805, https://doi.org/10.1016/j.ijmecsci.2021.106805.
[46] H. Wang, W. Shen, Y. Li, et al., Dynamic behavior and seismic performance of base-isolated structures with electromagnetic inertial mass dampers: analytical solutions and simulations, Eng. Struct. 246 (2021) 113072, https://doi.org/10.1016/j.engstruct.2021.113072.
[47] L. Chen, S. Nagarajaiah, L. Sun, A unified analysis of negative stiffness dampers and inerter-based absorbers for multimode cable vibration control, J. Sound Vib. 494 (2021) 115814, https://doi.org/10.1016/j.jsv.2020.115814.
[48] N. Ul Islam, R.S. Jangid, Seismic performance and control of elevated liquid storage tanks with negative stiffness and inerter-based dampers, Pract. Period. Struct. Des. Construct. 28 (3) (2023) 04023022.
[49] N.U. Islam, R.S. Jangid, Closed form expressions for H2 optimal control of negative stiffness and inerter-based dampers for damped structures, Structures 50 (2023, April) 791–809. Elsevier.
[50] N.U. Islam, R.S. Jangid, Optimum parameters and performance of negative stiffness and inerter based dampers for base-isolated structures, Bull. Earthq. Eng. 21 (3) (2023) 1411–1438.
[51] S. Elias, Effect of SSI on vibration control of structures with tuned vibration absorbers, Shock Vib. 2019 (2019) 1–12.
[52] A. Farshidianfar, S. Soheili, Ant colony optimization of tuned mass dampers for earthquake oscillations of high-rise structures including soil–structure interaction, Soil Dynam. Earthq. Eng. 51 (2013) 14–22.
[53] A. Farshidianfar, S. Soheili, ABC optimization of TMD parameters for tall buildings with soil structure interaction, Interact. Multiscale Mech. 6 (4) (2013) 339–356.
[54] R.N. Jabary, S.P.G. Madabhushi, Structure-soil-structure interaction effects on structures retrofitted with tuned mass dampers, Soil Dynam. Earthq. Eng. 100 (2017) 301–315.
[55] G. Bekdaş, S.M. Nigdeli, Metaheuristic based optimization of tuned mass dampers under earthquake excitation by considering soil-structure interaction, Soil Dynam. Earthq. Eng. 92 (2017) 443–461.
[56] J. Salvi, F. Pioldi, E. Rizzi, Optimum tuned mass dampers under seismic soil-structure interaction, Soil Dynam. Earthq. Eng. 114 (2018) 576–597.
[57] G. Bekdaş, A.E. Kayabekir, S.M. Nigdeli, Y.C. Toklu, Tranfer function amplitude minimization for structures with tuned mass dampers considering soil-structure interaction, Soil Dynam. Earthq. Eng. 116 (2019) 552–562.
[58] A. Farshidianfar, S. Soheili, Optimization of TMD Parameters for Earthquake Vibrations of Tall Buildings Including Soil Structure Interaction, 2013.
[59] O. Araz, K.F. Ozturk, T. Cakir, Effect of different objective functions on control performance of tuned mass damper for a high-rise building considering soil–structure interaction, Arch. Appl. Mech. 92 (4) (2022) 1413–1429.
[60] W. Zhang, S. Liu, M. Shokrabadi, A. Dehghanpoor, E. Taciroglu, Nonlinear seismic fragility assessment of tall buildings equipped with tuned mass damper (TMD) and considering soil-structure interaction effects, Bull. Earthq. Eng. 20 (7) (2022) 3469–3483.
[61] J.F. Wang, C.C. Lin, Seismic performance of multiple tuned mass dampers for soil–irregular building interaction systems, Int. J. Solid Struct. 42 (20) (2005) 5536–5554.
[62] C. Li, B. Han, Effect of dominant ground frequency and soil on multiple tuned mass dampers, Struct. Des. Tall Special Build. 20 (2) (2011) 151–163.
[63] R.N. Jabary, G.S. Madabhushi, Tuned mass damper positioning effects on the seismic response of a soil-MDOF-structure system, J. Earthq. Eng. 22 (2) (2018) 281–302.
[64] O. Araz, Optimization of tuned mass damper inerter for a high-rise building considering soil-structure interaction, Arch. Appl. Mech. 92 (10) (2022) 2951–2971.
[65] S. Liu, Z. Lu, P. Li, W. Zhang, E. Taciroglu, Effectiveness of particle tuned mass damper devices for pile-supported multi-story frames under seismic excitations, Struct. Control Health Monit. 27 (11) (2020) e2627.
[66] O. Araz, S. Elias, F. Kablan, Seismic-induced vibration control of a multi-story building with double tuned mass dampers considering soil-structure interaction, Soil Dynam. Earthq. Eng. 166 (2023) 107765.
[67] S. Elias, Vibration improvement of offshore wind turbines under multiple hazards, Structures 59 (2024, January) 105800. Elsevier.
[68] F. Pioldi, J. Salvi, E. Rizzi, Refined FDD modal dynamic identification from earthquake responses with Soil-Structure Interaction, Int. J. Mech. Sci. 127 (2017) 47–61.
[69] S. Gaur, S. Elias, T. Höbbel, V.A. Matsagar, K. Thiele, Tuned mass dampers in wind response control of wind turbine with soil-structure interaction, Soil Dynam. Earthq. Eng. 132 (2020) 106071.
[70] L. Luzi, G. Lanzano, C. Felicetta, M.C. D Amico, E. Russo, S. Sgobba, F. Pacor, ORFEUS Working Group 5, Engineering strong motion database (ESM) (version 2.0), Istituto Nazionale di Geofisica e Vulcanologia (INGV) (2020), https://doi.org/10.13127/ESM.2.
[71] S. Elias, R. Rupakhety, S. Ólafsson, Tuned mass dampers for response reduction of a reinforced concrete chimney under near-fault pulse-like ground motions, Frontiers in Built Environment 6 (2020) 92.
[72] R. Rupakhety, S. Elias, S. Olafsson, Shared tuned mass dampers for mitigation of seismic pounding, Appl. Sci. 10 (6) (2020) 1918.

[73] R. Rupakhety, Contemporary Issues in Earthquake Engineering Research: Processing of Accelerometric Data, Modelling of Inelastic Structural Response, and Quantification of Near-Fault Effects (Doctoral Dissertation), 2010.
[74] G.Ö. Sigurðsson, R. Rupakhety, S.E. Rahimi, S. Olafsson, Effect of pulse-like near-fault ground motions on utility-scale land-based wind turbines, Bull. Earthq. Eng. 18 (2020) 953–968.
[75] J. Salvi, F. Pioldi, E. Rizzi, Optimum tuned mass dampers under seismic soil-structure interaction, Soil Dynam. Earthq. Eng. 114 (2018) 576–597.